THE JOURNAL OF BIOLOGICAL CHEMISTRY VOL. 289, NO. 22, pp. 15426–15440, May 30, 2014

Neurolysin Knockout Mice Generation and Initial Phenotype Characterization*[S]

Received for publication, November 29, 2013, and in revised form, April 7, 2014 Published, JBC Papers in Press, April 9, 2014, DOI 10.1074/jbc.M113.539148

Diogo M. L. P. Cavalcanti[‡1,2], Leandro M. Castro[§¶1,3], José C. Rosa Neto[‡], Marilia Seelaender[‡], Rodrigo X. Neves[‡], Vitor Oliveira[¶3], Fábio L. Forti[‖], Leo K. Iwai[**], Fabio C. Gozzo[‡‡], Mihail Todiras[§§], Ines Schadock[§§], Carlos C. Barros[§§¶¶], Michael Bader[§§], and Emer S. Ferro[§3,4]

From the Departments of [‡]Cell Biology and Development and [§]Pharmacology, Support Center for Research in Proteolysis and Cell Signaling, Biomedical Sciences Institute, University of São Paulo, São Paulo, SP 05508-900, Brazil, the [¶]Department of Biophysics, Federal University of São Paulo, São Paulo, SP 04039-032, Brazil, the [‖]Department of Biochemistry, Support Center for Research in Proteolysis and Cell Signaling, Institute of Chemistry, University of São Paulo, São Paulo, SP 05508-000, Brazil, the [**]Special Laboratory of Applied Toxinology, Center of Toxins, Immune Response and Cell Signaling, Butantan Institute, São Paulo, SP 05503-000, Brazil, the [‡‡]Institute of Chemistry, State University of Campinas, Campinas, SP 13083-862, Brazil, the [§§]Max-Delbrück-Center for Molecular Medicine, D-13125, Berlin, Germany, and the [¶¶]Department of Nutrition, Federal University of Pelotas, Pelotas, RS 96010-610, Brazil

Background: Neurolysin is known to cleave several bioactive peptides *in vitro*.
Results: Neurolysin knock-out mice showed increased glucose tolerance, insulin sensitivity, and gluconeogenesis, which likely relates to increased expression of both specific liver mRNAs and intracellular peptides.
Conclusion: Neurolysin plays a role in energy metabolism.
Significance: Neurolysin could be used as a therapeutic target to counteract insulin resistance.

The oligopeptidase neurolysin (EC 3.4.24.16; Nln) was first identified in rat brain synaptic membranes and shown to ubiquitously participate in the catabolism of bioactive peptides such as neurotensin and bradykinin. Recently, it was suggested that Nln reduction could improve insulin sensitivity. Here, we have shown that Nln KO mice have increased glucose tolerance, insulin sensitivity, and gluconeogenesis. KO mice have increased liver mRNA for several genes related to gluconeogenesis. Isotopic label semiquantitative peptidomic analysis suggests an increase in specific intracellular peptides in gastrocnemius and epididymal adipose tissue, which likely is involved with the increased glucose tolerance and insulin sensitivity in the KO mice. These results suggest the exciting new possibility that Nln is a key enzyme for energy metabolism and could be a novel therapeutic target to improve glucose uptake and insulin sensitivity.

Neurolysin (EC 3.4.24.16; Nln)[5] is a zinc metalloendopeptidase with a conserved HE*XX*H motif. Nln was first identified in synaptic membranes of the rat brain by the specific cleavage and inactivation of the peptide neurotensin at the Pro-Tyr bond (1–3). Nln is a monomeric protein with a molecular mass of 78 kDa and 704 amino acid residues that hydrolyzes only peptides containing 5–17 amino acids by cleaving at a limited set of sites that are nonetheless diverse in sequence (4–9). The specificity of Nln for small bioactive peptide substrates without bulky secondary and tertiary structures is due to the presence of large structural elements erected over its active site region that allow substrate access only through a deep narrow channel (10). It is well established by biochemical analyses *in vitro* that Nln cleaves a number of bioactive peptides including neurotensin, bradykinin, hemopressin, and several opioid peptides at sequences that vary widely (5, 10, 11).

Nln is widely distributed in mammalian tissues and is found in different subcellular locations that vary with cell type (12–14). Much of the enzyme is cytosolic, but it also can be secreted or associated with the plasma membrane (12, 14), and some of the enzyme is synthesized with a mitochondrial targeting sequence by initiation at an alternative transcription start site (5, 15). Light and electron microscopic immunohistochemical studies have indicated that within the brain, Nln is present in both neurons and glia (12–14, 16). Studies in the neuroendocrine cell line AtT-20 have shown that Nln is enriched in the regulated secretory pathway (17). Nln was also shown to be released from glial cells in culture (14). The mechanism underlying Nln release is unclear, however, because the enzyme has no signal peptide or a hydrophobic membrane-spanning

* This work was supported by the Brazilian National Research Council Grants 559698/2009-7 (Rede GENOPROT), by Fundação de Amparo à Pesquisa do Estado de São Paulo Projeto Temático 04/04933-2 (to E. S. F.), and by the Pro-Reitoria de Pesquisa, University of São Paulo through Support Center for Research in Proteolysis and Cell Signaling Process 2012.1.17607.1.2.
[S] This article contains supplemental Tables S1–S5 and Fig. S1.
[1] These authors contributed equally to this work.
[2] Supported by Brazilian National Research Council Ph.D. Fellowship GM/GD-140650/2010-5 and SWE-200678/2011-6.
[3] Supported by Brazilian National Research Council research fellowships.
[4] To whom correspondence should be addressed: Av. Prof. Lineu Prestes 1524, Sala 315, São Paulo, SP 05508-900, Brazil. Tel.: 55-11-3091-7493; Fax: 55-11-3091-7422; E-mail: eferro@usp.br.
[5] The abbreviations used are: Nln, neurolysin; ACE, angiotensin-converting enzyme; SDH, succinate dehydrogenase; COX, cytochrome oxidase; PGAM, phosphoglycerate mutase; CPSM, carbamoyl-phosphate synthase 1, mitochondrial; GTT, glucose tolerance test; ITT, insulin tolerance test; qPCR, quantitative PCR; GO, Gene Ontology; PPPI, physical protein-protein interaction; ANOVA, analysis of variance; ESI, electrospray ionization; TMAB, 4-trimethylammoniumbutyryl.

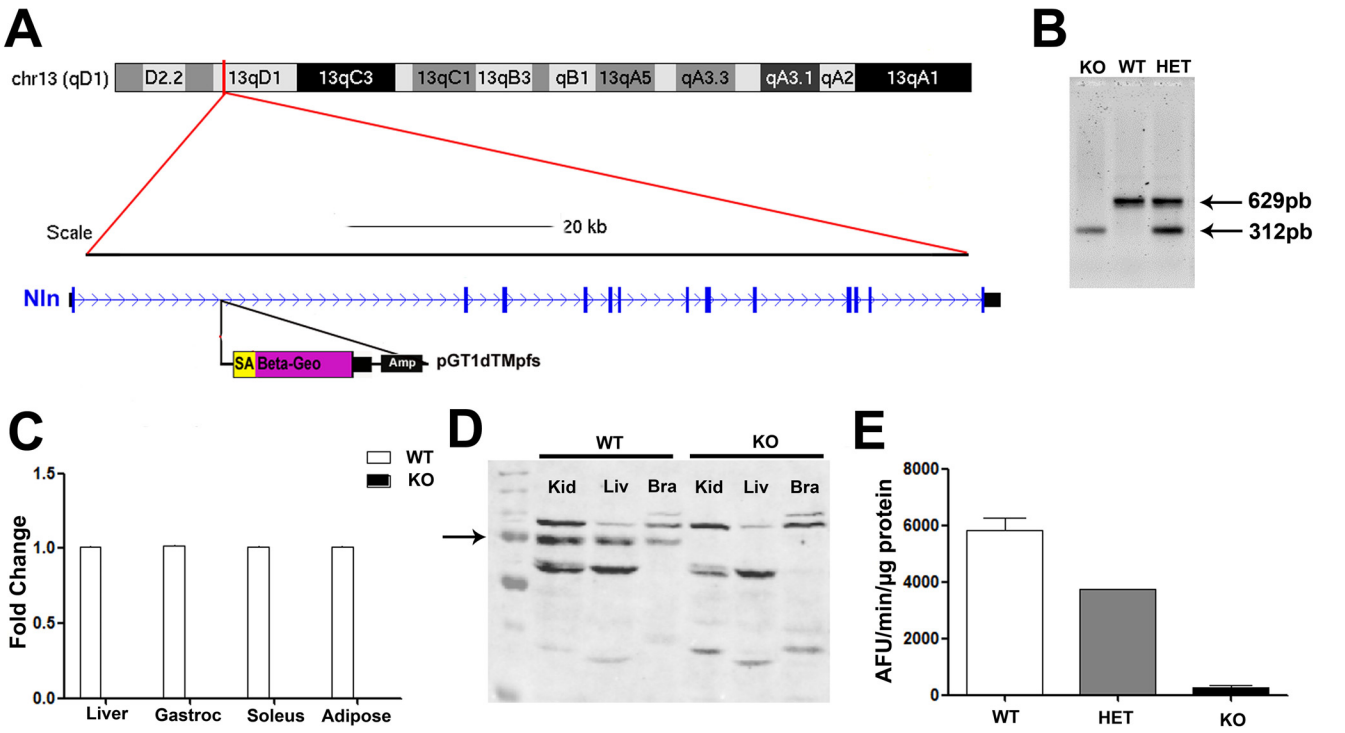

FIGURE 1. **Generation of Nln knock-out mice.** *A*, representation of Nln gene structure and the location of the NPX481 line gene trap insertion. The position of the Nln *locus* on a schematic representation of the mouse chromosome 13 is shown as a *red vertical line* (chr13-qD1). The Nln exons are represented as *blocks* connected by *arrowed lines*, where *blue blocks* indicate the coding, and *black blocks* indicate the untranslated regions. *B*, PCR for genotyping of Nln knock-out animals. *C*, qPCR showing absence of gene expression in KO animals in different tissues. *D*, Western blot showing Nln protein expression (*arrow*) in different organs (kidney, liver, and brain) in WT and KO. *E*, enzyme activity confirming the results of the genotyping and qPCR. *HET*, heterozygous; *Kid*, kidney; *Liv*, liver; *Bra*, brain; *ND*, not detected.

domain (14, 18). *In vivo* Nln has been suggested to be implicated in pain control (19–21), blood pressure regulation (22, 23), sepsis (24), reproduction (25, 26), cancer biology (27), and pathogenesis of stroke (28).

Previous studies suggested the involvement of proteases, peptidases, and peptides in metabolic disorders such as insulin resistance, obesity, and metabolic syndrome (29–32). For instance, carboxypeptidase E knock-out mice ($Cpe^{fat/fat}$) show an obesity phenotype (33, 34), and dipeptidyl peptidase 4-deficient mice are resistant to developing adiposity and obesity induced by high fat diet and exhibit improved insulin sensitivity (29, 30). Nln activity is significantly lower in the fat tissue of transgenic mice that are possessed three copies of the angiotensin-converting enzyme (ACE) gene. When these mice were fed a high fat diet, they showed better preserved insulin sensitivity compared with the group containing a single copy of the ACE gene (35). The reduced Nln activity in animals containing three copies of the ACE gene seem to correlate with a distinctive intracellular peptide profile of these animals; these results suggested that intracellular peptides could improve insulin sensitivity in the adipose tissue (35). Moreover, additional peptidomic studies using semiquantitative LC-MS/MS have shown that the intracellular levels of two of ten intracellular peptides found in the epididymal adipose tissue of animals, were at least two times higher in rats fed with a hypercaloric diet when compared with a control group. Indeed, if added back into 3T3-L1 adipocytes, these intracellular peptides significantly increased glucose uptake, corroborating the suggestion that intracellular peptides may be functional and regulate insulin signal transduction and glucose uptake in the adipose tissue (35, 36).

Here, Nln KO mice were generated to allow further investigation on the biological function of this peptidase in energy metabolism. Our initial phenotype characterization of KO mice seem to corroborate previous suggestions that Nln plays a physiological role in energetic balance increasing glucose tolerance, insulin sensitivity, and liver gluconeogenesis. However, although one cannot exclude compensatory mechanisms for a subset of Nln-associated phenotypes, we did not observe a key role of this oligopeptidase in blood pressure regulation.

EXPERIMENTAL PROCEDURES

Generation of Nln Knock-out Mice—The Nln gene trap knock-out mouse strain was generated by C57BL/6 blastocyst microinjection of genetically modified embryonic stem cells (NPX481, 129ola) obtained from Baygenomics through the International Gene Trap Consortium. The genetically modified Nln allele of the NPX481 strain has the gene trap vector pGT1dTMpfs inserted between exon 1 and exon 2 (Fig. 1*A*), as evidenced by sequencing 5′-rapid amplification of cDNA ends cDNA from the original NPX481 embryonic stem cell line (CC178547) used to generate this mice strain (a detailed report about this embryonic stem cell line can be found at the International Gene Trap Consortium website).

After transmission of the knock-out allele from chimera to F1 generation, Nln mice were obtained from heterozygous breeding, and the line was further maintained on the mixed

background by breeding $Nln^{+/-}$ with $Nln^{+/-}$ animals. To obtain such mice on a pure genetic background, we bred F1 (129/OlaHsd/C57BL/6 background) heterozygous Nln-deficient animals to the inbred C57BL/6 mouse line (Charles River) for 10 generations before using them for experimental investigations.

The mice were maintained in individual ventilated cages (Tecniplast Deutschland) under standardized conditions with an artificial 12-h dark-light cycle, with free access to standard chow (Ssniff) and drinking water *ad libitum*. The experiments were performed with adult mice (24 weeks old). This study was approved by the Ethics Committee of Institute of Biomedical Sciences at the University of São Paulo (protocol register number 44, page 86).

Genotyping—Genotyping of animals was performed using PCR with primer NlnF3 (5′-CGCCTCCTGCACCTACCA), pNlnwtR3 (5′-ATTTGCCAGGTTAAGAGATCG), and pNlnkoR2 (5′-CGTGTCCTACAACACACACTCC). The absence of Nln transcripts in the liver, muscle, and adipose tissue of Nln-deficient animals was confirmed by qPCR with the primer pair Nln-Fw (5′-CTGAAGGCCTGCTAAGCATC-3′) and Nln-Rv (5′-CGCATGGTTGTATTTTCCT-3′).

Enzymatic Activity—The enzymatic activity of Nln was determined in triplicate using a continuous assay with a quenched fluorescent substrate (7-methoxycoumarin-4-acetyl-P-L-G-P-dK-(2,4-dinitrophenyl) as previously described (5). The Nln specific inhibitor Pro-Ile (5 mM) (37) was used to discern the peptidolytic activity attributed exclusively to Nln. The results were expressed as arbitrary units of fluorescence per minute normalized by protein concentration.

Body Composition—Body composition (free water, fat, and lean mass) was estimated in 6-month-old mice by dual energy x-ray absorptiometry using a Hologic QDR 4500 scanner (Hologic, Waltham, MA) as described previously (38).

GTT, ITT, and Gluconeogenesis—Mice were fasted for 12 h, and blood samples were taken before and 15, 30, 60, 90, and 120 min after the injection of 2 g/kg glucose (GTT) or 0.75 unit/kg insulin (ITT). Gluconeogenesis was assessed by injecting 2 g/kg sodium pyruvate after 16 hof fasting. In all three assays, glycemia was measured using a glucometer (Accu-Check Performa; Roche).

Western Blot—For determining insulin signaling *in vivo*, we collected samples of muscle, liver, and epididymal adipose tissue before and 5 min after tail vein injection of insulin (5 units/kg) as previously described (39). The samples were immediately stored in liquid nitrogen.

For Western blot analyses, tissue lysates were homogenized in radioimmune precipitation assay buffer containing inhibitors of proteases (Complete; Roche) and phosphatases (PhosSTOP; Roche). Samples were subjected to SDS-PAGE in a Bio-Rad electrophoresis apparatus (Mini-Protean). Proteins were transferred to a PVDF membrane (Thermo Scientific Pierce). After 2 h in blocking buffer (Odyssey; LI-COR Biosciences), the membranes were incubated with anti-Nln (rabbit polyclonal antibody; Abcam), anti-phospho-AKT (Ser-473), or anti-AKT (rabbit polyclonal antibody; Cell Signaling) overnight at 4 °C and then incubated with IRDye secondary antibody (Odyssey; LI-COR Biosciences). The results were visualized in an Odyssey infrared imaging system (Odyssey; LI-COR Biosciences) and was quantified by densitometry with Odyssey infrared imaging software (Odyssey; LI-COR Biosciences).

Histological Analysis—We performed hematoxylin and eosin staining for histological analysis in gastrocnemius, soleus, liver, and adipose tissue. For mitochondrial activity, we used a tetrazolium compound and 3,3′-diaminobenzidine to identified sites for succinate dehydrogenase (SDH) and cytochrome oxidase (COX), respectively, in fresh frozen sections of gastrocnemius, as previously described (40, 41). All data acquisition and analysis were performed in a microscopy BZ-9000 (BIOREVE).

Real Time PCR—We used real time qPCR to determine mRNA expression in liver, muscle, and adipose tissue. Animals fasted for 12 h were sacrificed by decapitation, and tissues were removed, snap frozen in liquid nitrogen, and stored in −80 °C until use. Samples were homogenized, and total RNA was isolated using TRIzol protocol (TRIzol® products; Invitrogen). The total RNA was cleaned in a RNeasy mini kit (Qiagen), and the RNA integrity was assessed by electrophoresis on 1% agarose gels.

cDNA was synthesized from 1 μg of total RNA with Moloney murine leukemia virus reverse transcriptase (Invitrogen) using random hexamer nucleotides. Standard curves for all primers were made to determine the amplification efficiencies of target and reference genes. Quantitative PCR was performed on an ABI Prism 7900 (Applied Biosystems) sequence detection system with 100 nM primers and 20 ng of cDNA. Target mRNA expression was normalized to GAPDH expression and expressed as a relative value using the comparative threshold cycle (Ct) method ($2^{-\Delta\Delta Ct}$) according to the manufacturer's instructions. Expression levels from genes of interest were normalized to WT control mice and presented as fold change. All primers sequences used herein are described in supplemental Table S1.

Graded Treadmill Exercise Test—Exercise capacity, estimated by total distance run, correlates with skeletal muscle work capacity. Exercise capacity was evaluated with a graded treadmill using protocols from previously published reports. Briefly, after being adapted to treadmill exercises over a week (10 min of exercise per session); mice were placed in the treadmill streak and allowed to acclimatize for at least 30 min. We used high and low intensity running regimens. For high intensity running, intensity of exercise was increased by 3 m/min every 3 min until exhaustion. Exhaustion was defined as the time when animals were unable to keep pace with the treadmill for up to 1 min. For low intensity running, we used the average speed in the high intensity running and calculated 70% of this result (21m/min) and put all animals to run in this constant speed until exhaustion for maximum capacity of physical exercise.

Blood Pressure—Measurement of blood pressure was performed as previously described (42). KO and WT were anesthetized with isoflurane and then a modified catheter (type MRE: 0.25-inch outer diameter and 0.012-inch inner diameter; Braintree Scientific, Braintree, MA) was placed into the abdominal aorta via the femoral artery for measurement of arterial blood pressure. The blood pressure was measured using a transducer (MLT 1050 model) connected to a computer system for data

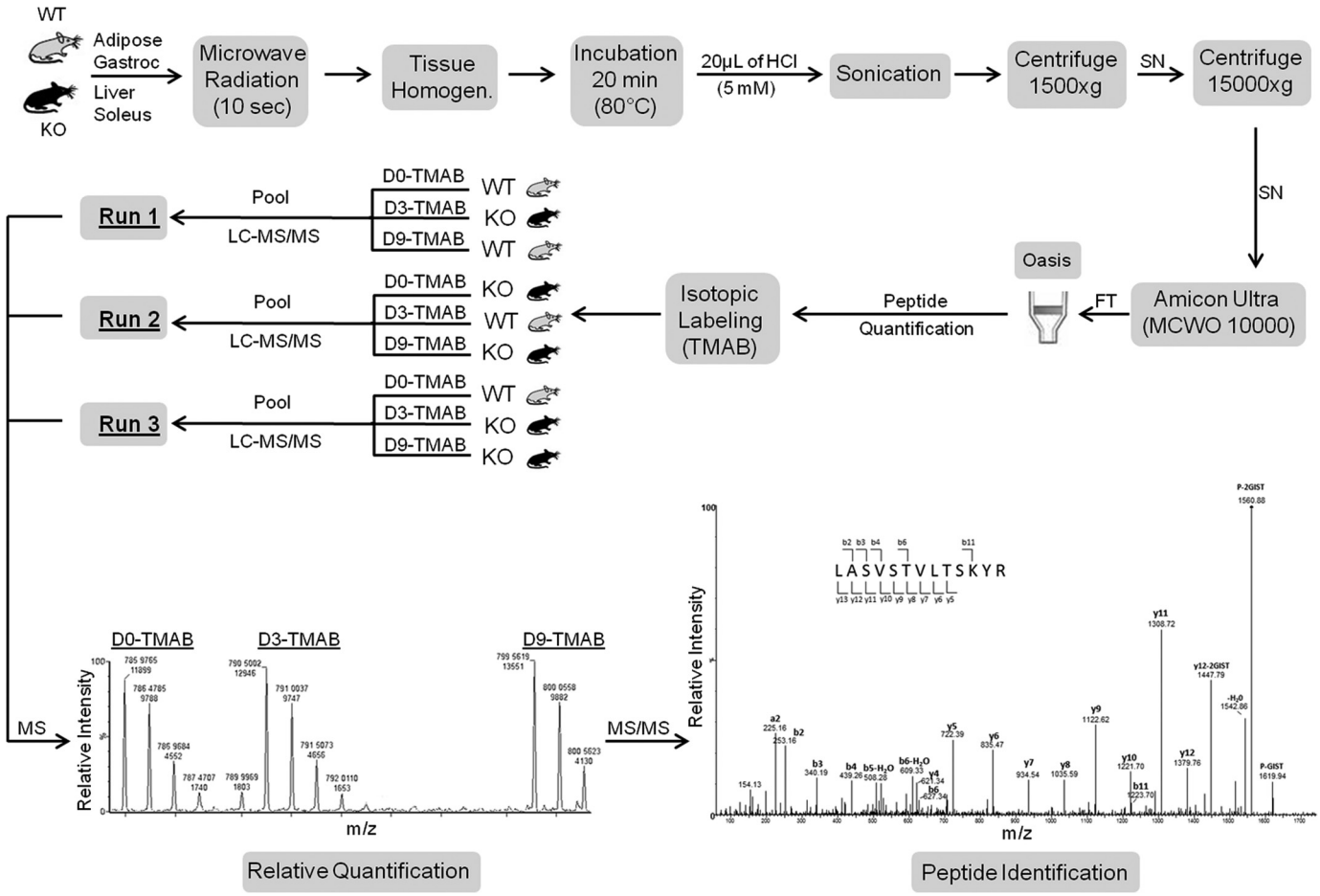

FIGURE 2. **Scheme for intracellular peptide extraction, labeling, and LC-MS/MS analysis.** First, the scheme shows briefly step by step the protocol for intracellular peptide extraction. For isotopic labeling with TMAB, we used three isotopic tags for each replicate. Intracellular peptides extracted from adipose tissue, gastrocnemius, liver, and soleus were labeled with D0-TMAB, D3-TMAB, and D9-TMAB and pooled as indicated in three different runs. The runs were labeled with reverse isotopic tags as control of the reactivity. The relative quantification is performed by measuring the intensity of the peak of peptide labeling with each isotopic tag from MS, taking an average of these values, and comparing the ratio of KO to the WT. For peptide identification, the MS/MS spectra were analyzed with a Mascot program to identify the sequences followed by manual interpretation to eliminate false positives.

analysis (PowerLab; AD Instruments, Colorado Springs, PA) (43). To test blood pressure response to different drugs (1 nM neurotensin, 5 and 10 mg/kg bradykinin, and 100 ng/kg angiotensin II), a second modified catheter was placed in the femoral vein.

Peptide Extraction—Peptide extracts were prepared as previously described (44, 45). Briefly, 6-month-old mice male ($n = 5$) were sacrificed by decapitation, and gastrocnemius, soleus, liver and epididimal adipose tissue were collected and subjected to 10 s of microwave (1500 watts; Electrolux) radiation to inactivate protein and peptide degradation. Each sample was homogenized (Polytron; Brinkmann) in 10 ml of water and incubated at 80 °C for 20 min. After cooling on ice, 20 µl of 5 M HCl was added to give a final concentration of 10 mM and sonicated three times with 20 pulses (4 Hz). The homogenates were centrifuged at 1,500 × *g* for 40 min at 4 °C. After this point, the supernatants were collected and centrifuged at 15,000 × *g* for 40 min at 4 °C. The resulting supernatants were collected and filtered through a Millipore membrane (molecular weight cut-off = 10,000; Amicon Ultra™; Millipore). The flow-through was applied to C18-like Oasis columns (Waters) (Fig. 2). The peptide extracts were resuspended in 100 µl of deionized water and kept at −80 °C.

Peptide Quantification—Peptide concentration was determined as previously described (44, 46). The reaction was performed at pH 6.8 to ensure that only the amino groups of peptides and not those of free amino acids react with fluorescamine (47). Briefly, 2.5 µl of each sample was mixed with 25 µl of 0.2 M phosphate buffer (pH 6.8) and 12.5 µl of a 0.3 mg/ml fluorescamine solution in acetone. After vortexing for 1 min, 110 µl of water was added, and fluorescence was measured with a SpectraMax M2^e plate reader (Molecular Devices) at an excitation wavelength of 370 nm and an emission wavelength of 480 nm. The peptide 5A (LTLRTKL), of known composition and concentration, was used as the standard reference for determining the peptide concentration.

Isotopic Labeling—The isotopic labeling of peptides for semiquantitation was performed as originally described (48, 49). Fifty micrograms of peptide extract from gastrocnemius, soleus, liver, or epididymal adipose tissue were combined with 200 µl of 0.4 M phosphate buffer, pH 9.5. The pH was adjusted to 9.5 with 1 M NaOH, 6.4 µl of a solution 350 µg/µl D0-TMAB, D3-TMAB, or D9-TMAB, dissolved in Me_2SO was added. After 10 min at room temperature, an appropriate volume of 1.0 M NaOH was added to the reaction mixture to adjust the pH back to 9.5, and the reaction was further incubated for 10 min. The

addition of labeling reagent and alkaline solution was repeated six times over 2 h, and the mixture was incubated at room temperature for 30 min. After incubation, 30 μl of 2.5 M glycine was added to the reaction to quench any remaining labeling reagent. After 40 min at room temperature, the hydrogen and deuterium samples were combined and centrifuged at 800 × *g* for 5 min at 4 °C. The pH was adjusted to 9.0–9.5, and 3 μl of 2.0 M hydroxylamine was added to remove TMAB labels from Tyr residues. The addition of hydroxylamine was repeated twice more over 30 min. The samples were desalted with a C18 column (Oasis Millipore, Billerica, MA). The peptides were applied to C18-like Oasis columns (Waters), eluted with 100% methanol, 015% trifluoroacetic acid, and dried in a vacuum centrifuge. Samples were resuspended in 10 μl of deionized water (Fig. 2).

Mass Spectrometry and MS and MS/MS Data Analyses—LC-MS/MS experiments were performed on a Synapt G2 QTOF mass spectrometer (Waters) as described previously (44). To identify peptides, the raw data files were converted to a peak list format (mgf) by Mascot Distiller version 2.1.1 (Matrix Science) and analyzed using the search engine MASCOT version 2.2 (Matrix Science). The SwissProt database was used for searches with taxonomy *Mus musculus*, "no enzyme," and 0.2 Da of mass tolerance for MS and MS/MS precursor ions. Mascot searches were followed by manual interpretation to eliminate false positives. Quantification was performed by measuring the ratio of peak intensity for the various TMAB-labeled peptide pairs in the MS spectra. For this analysis, the monoisotopic peak and the peaks containing one or two atoms of ^{13}C were used. Multiple scans of the MS spectra were combined prior to quantitation (Fig. 2).

Gene Ontology Analysis—The 40 proteins obtained from the peptidomic analyses shown in supplemental Table S3 plus Nln (shown in supplemental Table S4) were subjected to Gene Ontology (GO) clustering analysis using Biological Network Gene Ontology (BiNGO) software (50), a freely available plugin for the Cytoscape software, version 3.0.1 (51). The selected ontology file was based on Biological Process, the annotation file was based on *Homo sapiens* databanks, and the selected categories to be visualized discarded the evidence codes by overrepresentation after correction. The degree of functional enrichment for that list of proteins was obtained quantitatively (*p* value) with the hypergeometric distribution statistical test (52, 53), which worked independently inside of the BiNGO software application platform, and the corrected *p* value was obtained after applying false discovery rate control (85) correction with a significance level of 0.05. The selected reference test was the whole annotation from databases.

Construction of Physical Protein-Protein Interaction (PPPI) Networks—To design and construct a potential PPPI network containing Nln and the proteins represented by peptides from the peptidomic analyses shown in supplemental Table S3, we initiated data mining of human protein-protein interaction databases using them as a seed list. This procedure was carried out inside the Cytoscape platform with the APID2NET Cytoscape Plug-in software (54). The obtained network was named Union (because it was originated by the union of proteins identified in the gastrocnemius, liver, soleus, and adipose tissue samples), which was then submitted to GO analysis again, as above described.

Statistics—The values are expressed as means ± S.E. Statistical analyses were conducted by Student's unpaired *t* test for independent samples or ANOVA followed by Bonferroni's test to compare more than two groups. *p* values < 0.05 were considered significant.

RESULTS

Gene Trap Strategy for Knock-out of Nln Expression in Mice—The summarized strategy of generating Nln KO mice by insertion of a gene trap between exons 1 and 2 is illustrated in Fig. 1*A*. The presence of the gene trap in the Nln gene of the knock-out mice was confirmed by genotyping (Fig. 1*B*). To obtain a pure genetic background, we bred F1 heterozygous Nln-deficient animals to the C57BL/6 mouse line for 10 consecutive generations. After 10 generations, the Nln mRNA, protein levels and enzymatic activity were investigated in various tissues, confirming the absence of Nln mRNA and protein expression in these KO mice (Fig. 1, *C–E*).

Initial Phenotypical Characterization of Nln Knock-out Mice—Disruption of Nln expression caused neither embryonic lethality nor changes in the normal Mendelian distribution following intercrossing of the heterozygotes. KO mice could not be visually distinguished from WT C57BL/6 littermates and had normal external appearance and fertility. KO and WT mice also showed similar muscle mass, free water, and fat mass composition as analyzed by densitometry (Fig. 3, *A–C*). In contrast, KO mice showed a slight although statistically significant ($p < 0.05$) ~10% decrease in body weight compared with WT (Fig. 3*D*); however, no difference in the specific mass of the internal organs was observed (supplemental Table S2). There was also no obvious difference in the morphology of skeletal muscle, liver, and epididymal adipose tissue stained with hematoxylin and eosin1 (Fig. 3, *E–J*).

Insulin Sensitivity and Gluconeogenesis Tests—The basal glucose levels of WT and KO are similar (Fig. 4*A*). However, the intraperitoneal GTT done in WT and KO fasted for 12 h shows lower glucose concentrations at 15, 30, 60, and 90 min in KO compared with WT (Fig. 4, *B* and *C*). To further assess insulin sensitivity, we performed the ITT in 12-h-fasted mice. Considering the normalized curve for the ITT data (Fig. 4*D*) and the constant rate for glucose disappearance (K_{ITT}; Fig. 4*E*), KO showed an increase of insulin sensitivity when compared with WT. The liver gluconeogenesis capacity of KO is higher compared with WT animals (Fig. 5, *A* and *B*), as shown by the intraperitoneal pyruvate tolerance test in animals fasted for 16 h.

Comparative analyses of several regulatory genes involved in liver gluconeogenesis were performed in WT and KO using qPCR. These results suggest that KO have increased liver mRNA for the *Fbp1* (fructose bisphosphatase 1), *PPARγ* (peroxisome proliferator-activated receptor γ), and *Creb1* (cAMP-responsive element-binding protein 1), and *Cox4i1*, which is in agreement with an increased liver gluconeogenesis of KO when compared with the WT animals (Fig. 5*C*).

Graded Treadmill Exercise Tests—WT and KO mice performance on a treadmill was evaluated in two different tests.

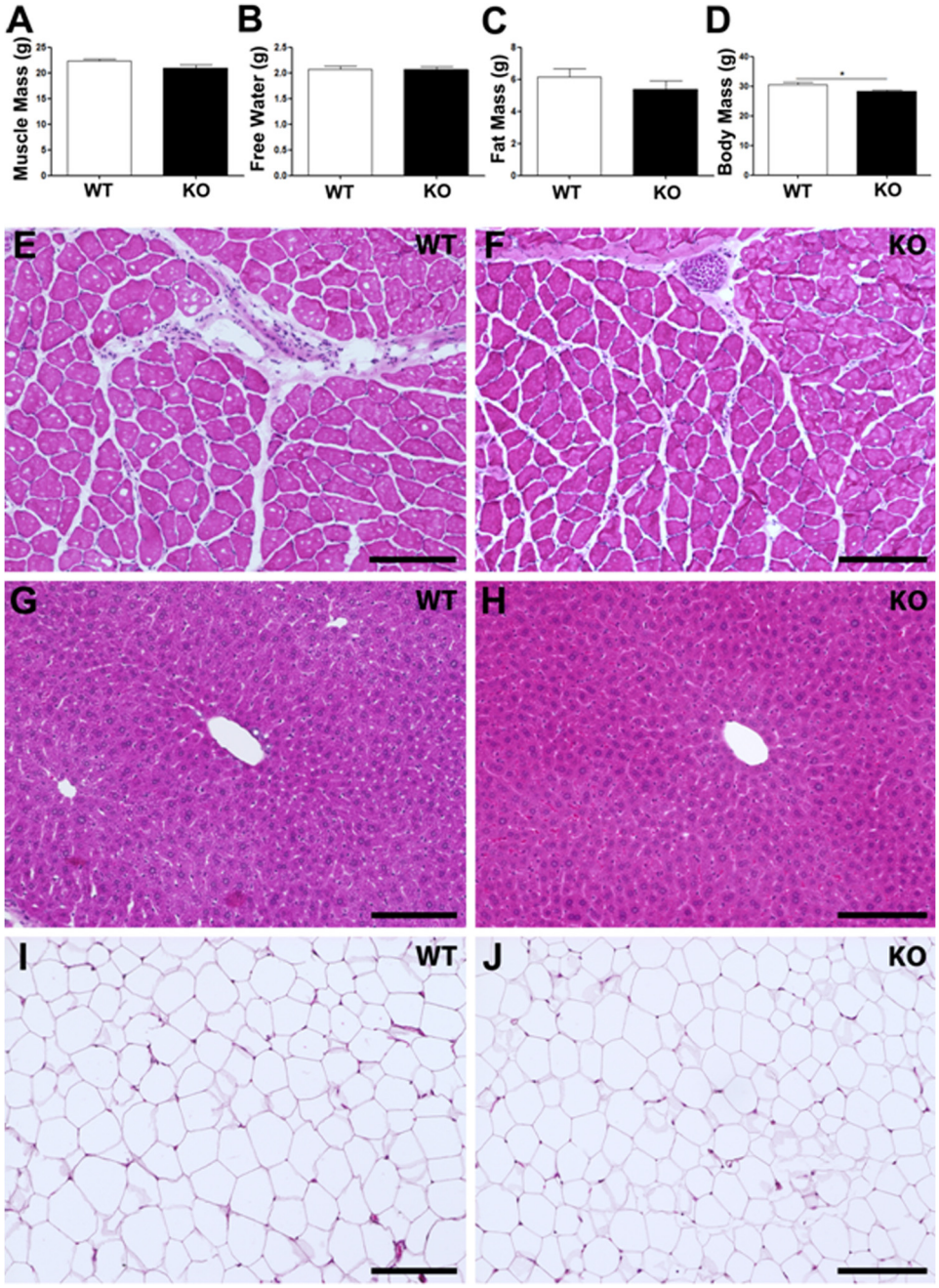

FIGURE 3. **Body weight, basal glucose levels, and body composition.** *A–C*, body composition of muscle mass (*A*), free water (*B*), and fat (*C*) ($n = 6$). *D*, average body weight of WT and 24-week-old KO animals ($n = 6$). The data are presented as means ± S.E. Student's unpaired *t* test was used. *, $p < 0.05$. *A–J*, histological analysis. *E* and *F*, muscle histological sections (gastrocnemius) stained with hematoxylin and eosin of 24-week-old WT and KO animals, respectively. *G* and *H*, liver histological sections stained with hematoxylin and eosin of 24-week-old WT and KO animals, respectively. *I* and *J*, epididymal adipose tissue histological sections stained with hematoxylin and eosin of 24-week-old WT and KO animals, respectively ($n = 5$).

First, animals were subjected to a high intensity running regime that increased the speed stepwise every 3 min up to the ratio of 3 m/min until exhaustion. These results showed no statistical difference between WT and KO animals (Fig. 6, A and B); on average, WT and KO mice ran 422 and 337 m, respectively, before complete exhaustion. Second, animals were subjected to a low intensity running regime (21 m/min constant) until exhaustion, and the KO (637 m) ran significantly (~36%) less when compared with WT (997 m) (Fig. 6, *C* and *D*), suggesting that Nln is linked to oxidative metabolic capacity and physical exercise endurance.

Molecular Basis of Increased Glucose Metabolism in KO Mice—To further investigate the molecular basis correlated with the higher insulin responsiveness in KO, we analyzed the insulin signal transduction pathway through $AKT^{Ser\text{-}473}$ phosphorylation in the gastrocnemius, liver, and epididymal adipose tissues of both WT and KO animals. Whereas the basal levels of $AKT^{Ser\text{-}473}$ phosphorylation were similar between WT and KO animals (Fig. 7, *A–C*), following a stimulus with an acute intravenous insulin injection, it was higher in gastrocnemius (Fig. 7*A*) and epididymal adipose tissue (Fig. 7*B*) but not in the liver (Fig. 7*C*) of KO compared with WT animals.

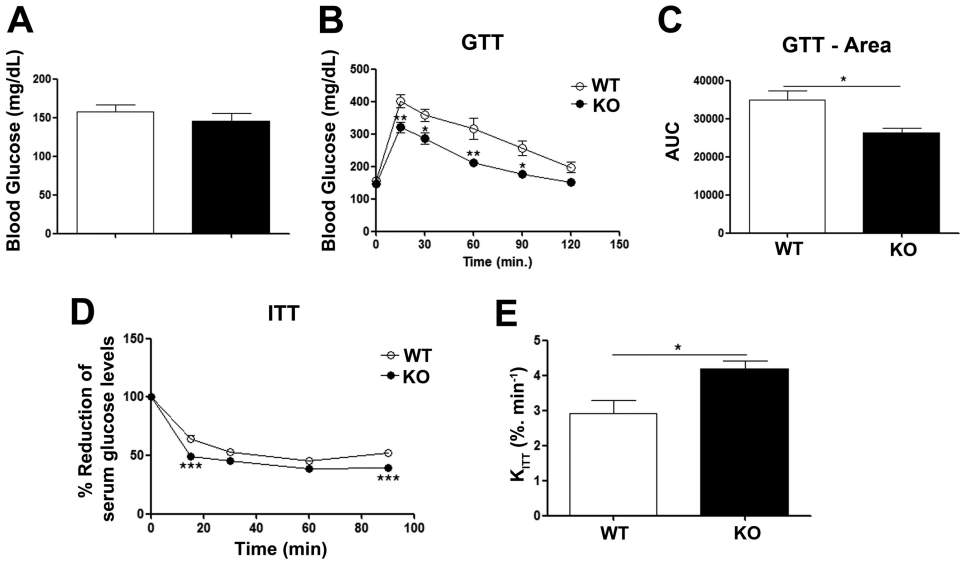

FIGURE 4. **Glucose and insulin tolerance test.** *A*, basal blood glucose levels after fasting for 12 h ($n = 6$). *B*, GTT after fasting for 12 h of 24-week-old WT and KO animals ($n = 6$). *C*, area under the curve (*AUC*) for the glucose tolerance test. *D*, after fasting for 12 h of 24-week-old WT and KO animals ($n = 6$). *E*, calculation of the constant of glucose disappearance (K_{ITT}) for the insulin tolerance test. The data are presented as means ± S.E. Student's unpaired *t* test or ANOVA followed by Bonferroni's test was used. *, $p < 0.05$; **, $p < 0.01$; ***, $p < 0.001$.

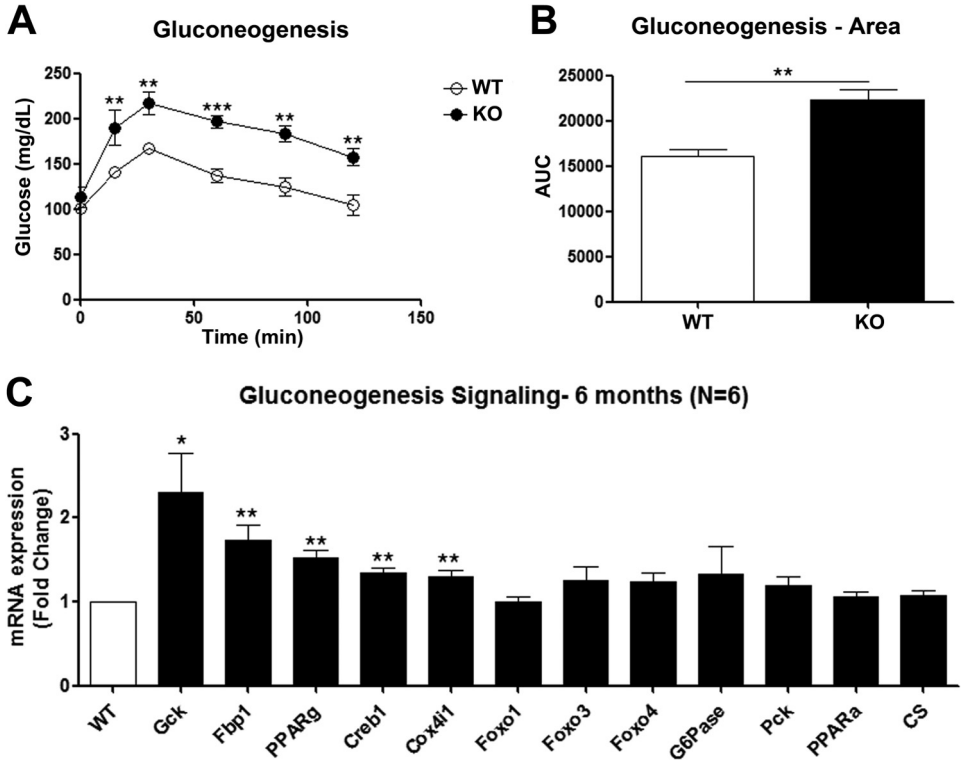

FIGURE 5. **Pyruvate tolerance test and hepatic gluconeogenesis regulatory enzymes.** *A*, pyruvate tolerance test of 24-week-old WT and KO animals to check the level of gluconeogenesis in the liver ($n = 6$). *B*, area under the curve for the pyruvate tolerance test. *C*, quantitative real time PCR for genes that are related to gluconeogenesis in the liver ($n = 6$). The data are presented as means ± S.E. Student's unpaired *t* test or ANOVA followed by Bonferroni's test was used. *, $p < 0.05$; **, $p < 0.01$; ***, $p < 0.001$. *AUC*, area under the curve.

Fast Twitch Type II Fibers Remodeling in Nln Knock-out Mice in Gastrocnemius—The enzymatic activity of Nln in WT gastrocnemius (predominantly fast twitch type II fibers) is approximately three times lower than in the soleus (predominantly slow twitch type I fibers), liver, or epididymal adipose tissues (Fig. 8). Based on this finding and because KO mice ran less than WT mice in the low intensity running regime until exhaustion, we decided to investigate a possible remodeling of fiber compositions in skeletal muscle. Using qPCR, we analyzed mRNA expression of specific genes for slow twitch type I (Tnni1, Tnnt1, Tnnc1, and Myh7) and fast twitch type II fibers (Tnni2, Pvalb, Myh1, Myh2, and Myh4) in gastrocnemius and soleus (Fig. 9, *A* and *B*). KO showed a decrease in mRNA expression typical for slow twitch type I fibers in gastrocnemius

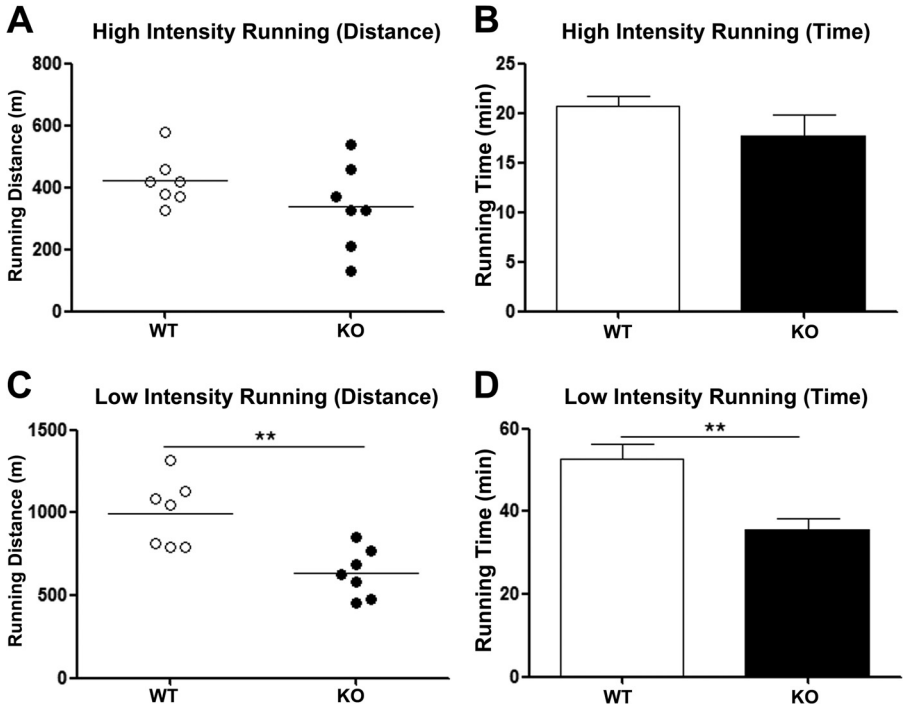

FIGURE 6. **Resistance and endurance running test.** *A*, running performance with high intensity individual and group average of 24-week-old WT and KO animals ($n = 7$). *B*, running time average of the high intensity test. *C*, running performance with low intensity individual and group average of 24-week-old WT and KO animals ($n = 7$). *D*, running time average of the low intensity test. The data are presented as means ± S.E. Student's unpaired *t* test was used. **. $p < 0.01$.

but not in soleus, whereas no differences were observed for fast twitch type II fibers in both skeletal muscles (Fig. 9, *A* and *B*).

Next, histological sections of gastrocnemius were stained for the mitochondrial enzymes SDH (Fig. 10, *A* and *B*) and COX (Fig. 10, *D* and *E*). Indeed, KO showed a significant decrease in the number of oxidative fibers (slow twitch type I) stained for both SDH (Fig. 10*C*) and COX (Fig. 10*F*) in the gastrocnemius tissue.

Distinctive Intracellular Peptide Profile of KO and WT in Skeletal Muscle, Liver, and Adipose Tissue—Semiquantitative peptidomic analyses using isotopic labeling and LC-ESI-MS were performed to identified possible differences in the global peptide profile between WT and KO animals (supplemental Table S3). Altogether, 736 MS peptide spectra were quantified including those peptides that were not sequenced by MS/MS (supplemental Table S3). All of these peptides were fragments of intracellular proteins, of which the relative levels seemed slightly affected by the lack of Nln. In accordance to previous reports (36, 44, 49), we postulated that Nln should be a key enzyme to metabolize peptides that have increased or decreased 2-fold (more than 100% of increase or more than 50% of decrease) in KO compared with WT mice; peptides that increase are considered potential Nln substrates, whereas peptides that decreased are considered potential Nln products. Thus, from the total of peptides identified (supplemental Table S3), only a small number could be considered either substrates or products of Nln (Table 1). In the gastrocnemius two peptides derived from troponin I, fast skeletal muscle, SADAMLKALLGSKHK and DMEVKVQKSSKELEDMNQKL, increased more than 2-fold (supplemental Table S1*B*). In the adipose tissue two different peptides, one derived from the acyl-CoA-binding protein (VEKVDELKKKYGI) and one derived from the hemoglobin subunit α (LASVSTVLTSKYR), increased more than 2-fold (supplemental Table S3*A*). In the liver, several endocannabinoid peptides containing the mouse hemopressin (PVNFKLLSH) endocannabinoid signature (SDLHAHKLRVDPVNFK, RVDPVNFKLLS, VDPVNFKLL, VDPVNFKLLSH, and RVDPVNF), or the previously identified antinociceptive AGH peptide (AGHLDDLPGALSA) decreased more than 2-fold (supplemental Table S3*C*). In the soleus, only the peptide FASFPTTK derived from the hemoglobin α subunit decreased more than 2-fold (supplemental Table S3*D*). None of the peptides identified in the gastrocnemius or in the epididymal adipose tissue decreased more than 2-fold. In liver and soleus tissues, none of the identified peptides increased more than 2-fold. Moreover, all the peptides identified here to change the relative concentration among KO and WT were in the size range of Nln substrate specificity, which are peptides containing ~5–20 amino acids. These data suggest a great specificity of Nln for metabolizing intracellular peptides and/or a compensatory mechanism occurring in the KO mice.

Nln Knock-out Mice Did Not Show Any Difference in Blood Pressure Parameters—A possible key role of Nln in degrading circulating bioactive peptides was first investigated through blood pressure monitoring, introducing a catheter in the femoral artery as previously described (42). Under basal conditions, WT and KO have similar mean arterial pressure (109.0 ± 1.5 *versus* 108.0 ± 1.5 mm Hg, respectively; Fig. 11*A*) and heart rate (668.4 ± 8.8 *versus* 652.0 ± 14.5 beats per min, respectively; Fig. 11*B*). Next, we challenged the participation of Nln in blood pressure regulation injecting vasoactive peptides such as bradykinin, neurotensin, and angiotensin II in two different doses (5 and 10 mg/kg). However, no significant differences were seen in the blood pressure effects of these peptides comparing WT to

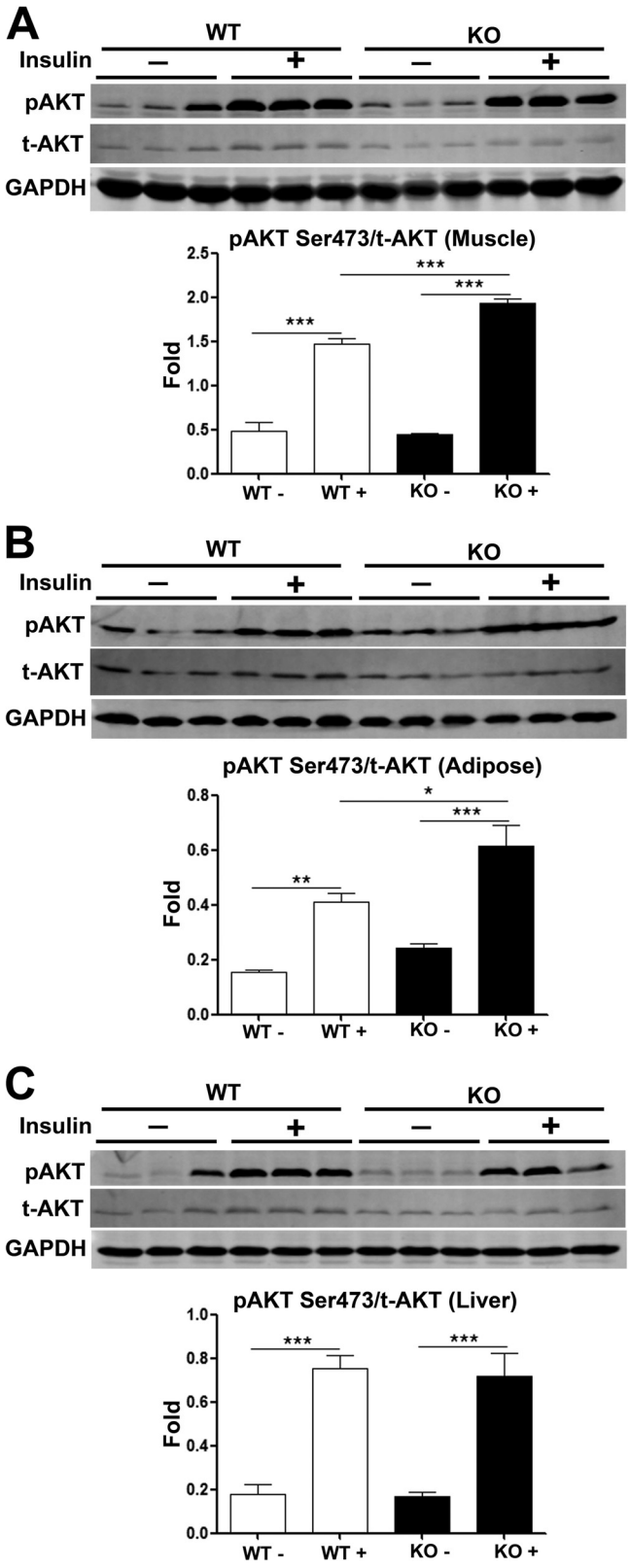

FIGURE 7. **AKT glucose signaling analysis by Western blotting.** *A–C*, Western blot showing AKT phosphorylation without (−) and with (+) insulin stimulation normalized to GAPDH in 24-week-old WT and KO animals ($n = 6$). *A*, muscle; *B*, adipose tissue; *C*, liver. Levels of AKT phosphorylation in each tissue are represented by the ratios of phosphorylated (*pAKT*) (Ser-473) to total (*t-AKT*). The data are presented as means ± S.E. ANOVA followed by Bonferroni's test was used. *, $p < 0.05$; **, $p < 0.01$; ***, $p < 0.001$.

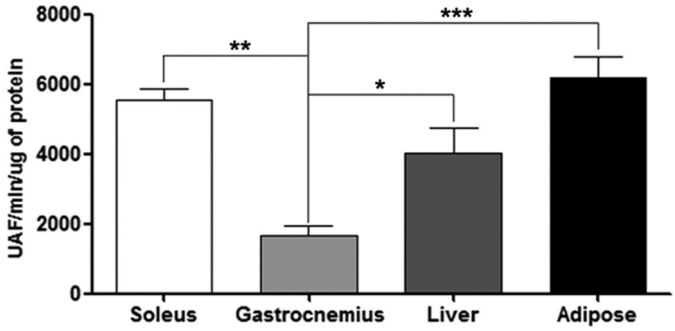

FIGURE 8. **Nln enzymatic activity in skeletal muscle, adipose tissue, and liver.** Shown are the levels of soleus (predominantly slow twitch type I fibers), gastrocnemius (predominantly fast twitch type II fibers), liver, and epididymal adipose tissue of C57BL/6 ($n = 3$). The data are presented as means ± S.E. ANOVA followed by Bonferroni's test was used. *, $p < 0.05$; **, $p < 0.01$; ***, $p < 0.001$. *UAF*, arbitrary units of fluorescence.

KO responses (Fig. 11, *C–E*). These data suggest that Nln alone is not a key enzyme in blood pressure regulation.

Gene Ontology Analysis and PPPI Networks—The intracellular peptides identified by LC-ESI-MS in the four peripheral tissues (adipose tissue, gastrocnemius, liver, and soleus) and shown in supplemental Table S3 were used to generate a list of thirty-nine proteins, which together with Nln itself were used for further *in silico* analysis (supplemental Table S4). To discover biological processes affected by the ablation of Nln, these proteins were submitted to GO analyses (Table 2), considering significant results only when the *p* value was below 10^{-5}. The list of biological process and genes related to these peptides are shown in Table 2. Most of the genes identified in the GO analyses are involved in basal energetic metabolism, such as glycolysis and glucose metabolism (ALDOA, G3PT, PGAM2, and CPSM) and muscle contraction (ALDOA, PGAM1, PGAM2, SMPX, and MYL1). qPCR analyses were performed to evaluate the effect of Nln KO in the expression of several of these genes, in the gastrocnemius and soleus (Fig. 12). These data suggest that Nln KO enhances CPSM and reduces PGAM1 and PGAM2 gene expression in the gastrocnemius, which is not observed in the soleus (Fig. 12).

Moreover, to identify other biological processes in which Nln might act as a direct or indirect regulator, we started data mining in physical protein-protein interaction databases by using as input the 40 proteins from supplemental Table S4 and constructed a network named Union (supplemental Fig. S1), because of the union of nonoverlapping proteins found in the gastrocnemius, liver, soleus, and adipose tissue samples, together with Nln. Despite the fact that a few proteins were not found in the human PPPI databases (used here because it is more complete and updated than the mouse database), the resulting network presented 229 proteins (nodes) and 680 connections, between the 40 input proteins and other related ones acting as substrates or interacting partners. In this complex network, Nln is initially not part of the biggest network (supplemental Fig. S1). However, as suggested by our results, Nln can interfere with other proteins, pathways, and biological processes. Thus, the obtained Union network was submitted to a new GO analysis, for enlarging the list of genes and biological processes that could be affected by the knock-out of Nln (supplemental Table S5). In addition to the general and tissue-

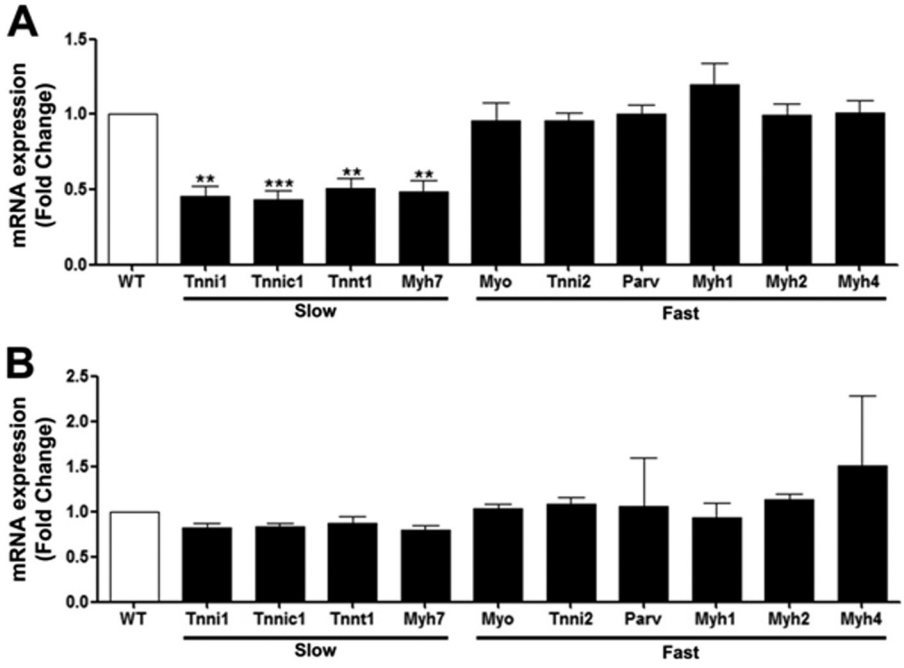

FIGURE 9. **Real time PCR analysis of type I/II specific gene and myosin heavy chain gene expression in different skeletal muscle.** *A*, quantitative real time PCR for specific genes from slow twitch type I fibers and fast twitch type II fibers in gastrocnemius ($n = 6$). *B*, quantitative real time PCR for specific genes from slow twitch type I fibers and fast twitch type II fibers in soleus ($n = 6$). The data are presented as means ± S.E. Student's unpaired *t* test was used. **, $p < 0.01$; ***, $p < 0.001$.

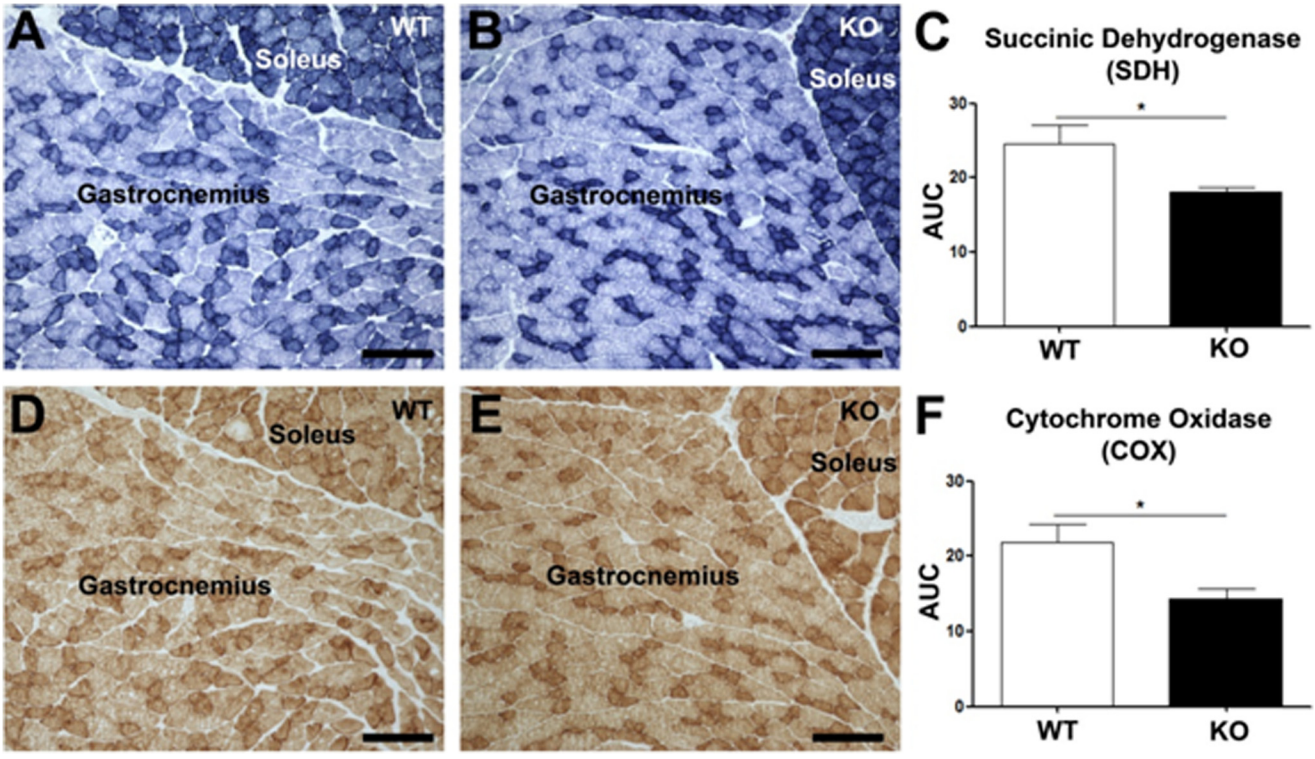

FIGURE 10. **Mitochondrial enzymatic activity in gastrocnemius.** *A* and *B*, muscle histological sections showing the SDH staining of 24-week-old WT and KO animals, respectively. *C*, relative quantification of histochemical succinate dehydrogenase staining ($n = 4$). *D* and *E*, muscle histological sections showing COX staining of 24-week-old WT and KO mice, respectively. *F*, relative quantification of histochemical cytochrome oxidase ($n = 4$). Note, stronger staining fibers are more oxidative (slow twitch type I), and light staining fibers are more glycolytic (fast twitch type II). The data are presented as means ± S.E. Student's unpaired *t* test was used. *, $p < 0.05$. *AUC*, area under the curve.

specific biological processes already found in Table 2, other biological processes related to the nervous system were also identified, such as: (*a*) regulation of nerve impulse transmission through synapses; (*b*) nervous system development; (*c*) learning and memory; (*d*) regulation of synaptic plasticity; (*e*) cell morphogenesis involving neuron differentiation; (*f*) response to different types of stressor agents; (*g*) DNA damage and repair pathways; (*h*) regulation of cell proliferation (S and M phases);

(*i*) intracellular signaling; and (*j*) protein stability, complex assembly, and post-translation modifications. Therefore, *in silico* analysis using a system biology approach (55), highlights Nln as a (indirect) regulator of several physiological and cellular processes in addition to energy metabolism. Further biological investigation is necessary to further validate these *in silico* data.

TABLE 1

Summary of intracellular peptides quantification by LC-ESI-MS

Global analysis of intracellular peptides profile in soleus (predominantly slow twitch type I fibers), gastrocnemius (predominantly fast twitch type II fibers), liver, and epididymal adipose tissue quantified by LC-ESI-MS as Nln substrate (ratio KO/WT ≥ 2.0), product (ratio KO/WT ≤ 0.5), or neither substrate or product (ratio KO/WT ≥ 0.5 and ≤ 2.0). The percentages indicate the amounts of intracellular peptides that are substrates, products, or not cleaved by Nln ($n = 5$).

	MS spectra	≥2.0 increased	≤0.5 decreased	≤0.5 and ≥2.0 not changed
Gastrocnemius	318	19 (6%)	0 (0%)	299 (94%)
Soleus	112	2 (2%)	8 (7%)	102 (91%)
Liver	189	2 (1%)	22 (12%)	165 (87%)
Adipose	110	15 (14%)	0 (0%)	95 (86%)

DISCUSSION

The major findings presented here are the generation and phenotype characterization of Nln KO mice. Nln was first described as a novel neurotensin-cleaving enzyme and received the first denomination of "neurotensin-degrading neutral metalloendopeptidase" (3). Whereas pharmacological studies have associated Nln to distinct physiological functions and several pathologies, one can reasonably argue that its actual physiological role is still elusive (56). Here, the characterization of Nln KO mice uncovered the physiological relevance for this oligopeptidase in the regulation of energy metabolism. Insulin resistance and diabetes type 2 are for a long time associated with increased cardiovascular risk factors, including dyslipidemia, hypertension, impaired fibrinolysis, coagulation, and obesity (57). Together with cardiovascular diseases, diabetes type 2 is one of the leading causes of mortality and mobility in the modern world (35). KO mice were shown here to have increased glucose tolerance, insulin sensitivity, and liver gluconeogenesis. Hence, these data suggest a novel therapeutic possibility, which

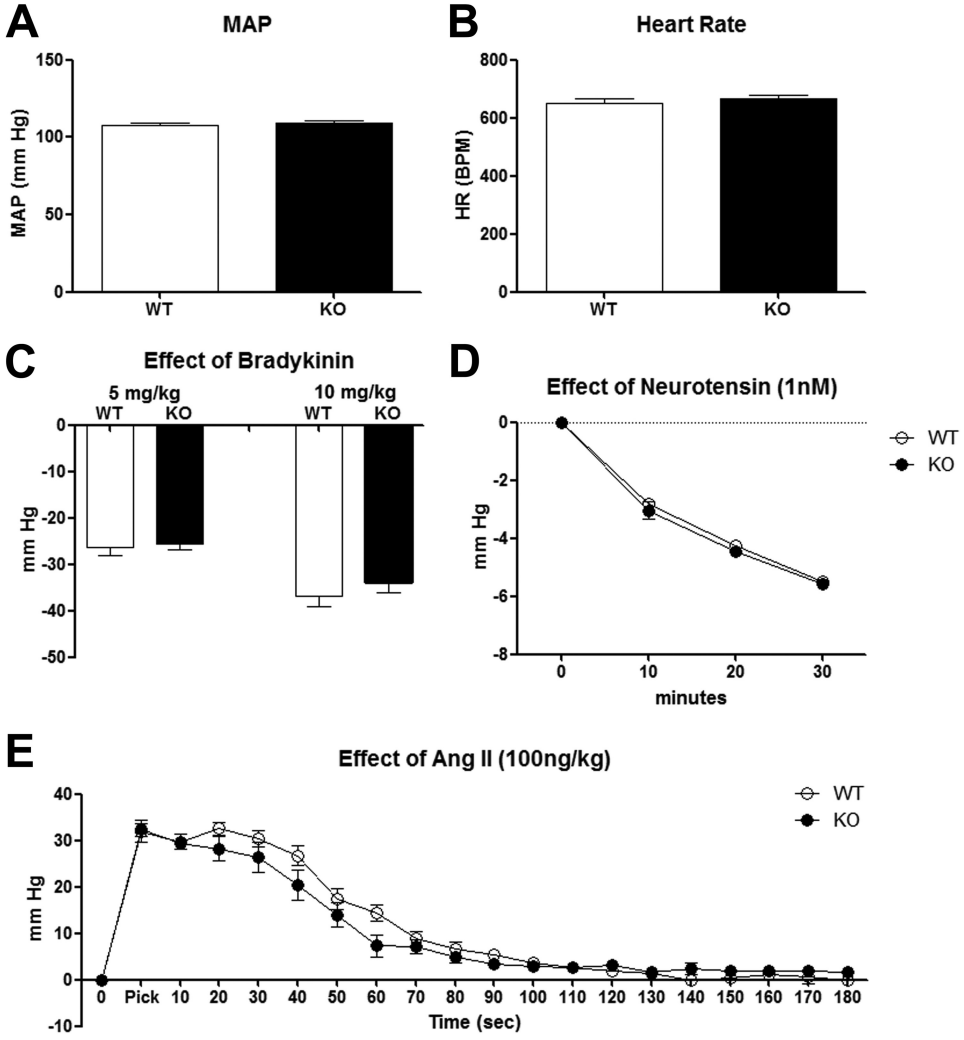

FIGURE 11. **Blood pressure.** *A* and *B*, mean arterial pressure (*A*, *MAP*) (expressed in mm Hg) and heart rate (*B*, expressed in beats per minute, *BPM*) measured by femoral artery catheterization compared KO and WT respectively ($n = 12$). *C*, effect of bradykinin on MAP after bradykinin injection in femoral vein (5 or 10 mg/kg) ($n = 7$). *D*, effect of neurotensin on MAP after neurotensin injection in femoral vein (1 nM/mice) ($n = 8$). *E*, time course of the effect of angiotensin II (*Ang II*) on MAP after angiotensin II injection in femoral vein (100 ng/kg) ($n = 8$). The data are presented as means ± S.E. Student's unpaired *t* test or ANOVA followed by Bonferroni's test shows no different statistical significance between groups.

TABLE 2
Gene Ontology (GO) obtained for the 40 proteins represented by the peptides identified in the gastrocnemius, soleus, liver, and adipose tissues, including the Nln

GO ID	*p* value	Biological process description	Genes in test set
6941	4,8E-20	Striated muscle contraction	ALDOA, PGAM2, TNNI2, SMPX, MYL1, MYG, and TNNT3
6936	4,8E-12	Muscle contraction	ALDOA, PGAM2, TNNI2, SMPX, MYL1, MYG, and TNNT3
3012	1E-11	Muscle system process	ALDOA, PGAM2, TNNI2, SMPX, MYL1, MYG, and TNNT3
3009	1,1E-08	Skeletal muscle contraction	TNNI2, MYG, and TNNT3
50881	1,2E-07	Musculoskeletal movement	TNNI2, MYG, and TNNT3
50879	1,2E-07	Multicellular organismal movement	TNNI2, MYG, and TNNT3
15671	2,9E-06	Oxygen transport	HBB and HBA
46461	9,6E-06	Neutral lipid catabolic process	APOA2 and CPSM
44269	9,6E-06	Glycerol ether catabolic process	APOA2 and CPSM
46464	9,6E-06	Acylglycerol catabolic process	APOA2 and CPSM
15669	1,9E-05	Gas transport	HBB and HBA
6110	2,1E-05	Regulation of glycolysis	PGAM1 and G3PT
46503	2,1E-05	Glycerolipid catabolic process	APOA2 and CPSM
6006	2,1E-05	Glucose metabolic process	ALDOA, PGAM2, CPSM, and G3PT
43471	6,8E-05	Regulation of cellular carbohydrate catabolic process	PGAM1 and G3PT
43470	6,8E-05	Regulation of carbohydrate catabolic process	PGAM1 and G3PT
44275	9,5E-05	Cellular carbohydrate catabolic process	ALDOA, PGAM2, and CPSM
19318	9,5E-05	Hexose metabolic process	ALDOA, PGAM2, CPSM, and G3PT

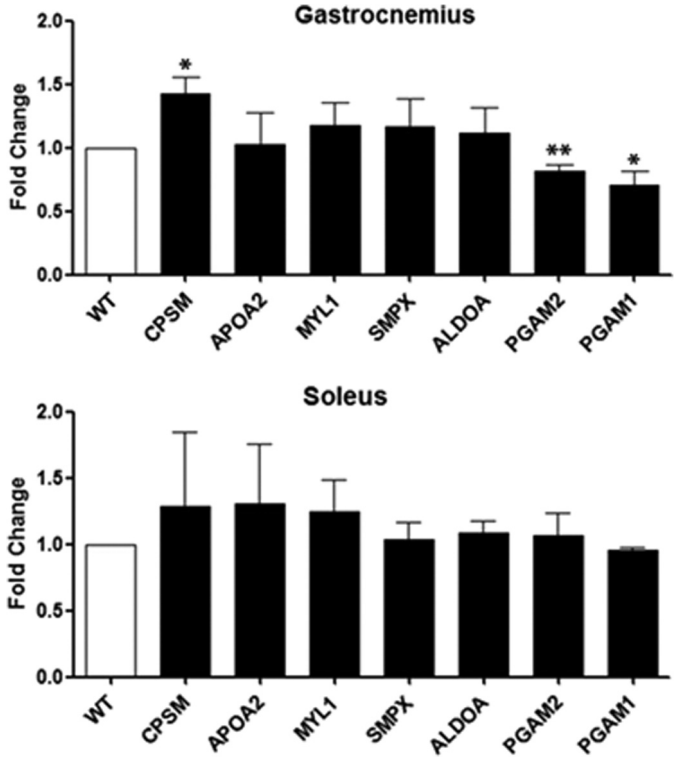

FIGURE 12. **qPCR for genes obtained after GO analyses.** qPCR in either WT (*white bars*) or KO (*black bars*) animals, both 24-week-old ($n = 4$). Several additional genes identified after GO to be related to muscle contraction, metabolic, and glucose metabolic process analyses were evaluated. *Upper panel*, gastrocnemius; *lower panel*, soleus. The data are represented as means ± S.E. Student's unpaired *t* test was used. *, $p < 0.05$; **, $p < 0.01$.

is to inhibit Nln for improving glucose uptake and peripheral insulin sensitivity.

Glucose metabolism is vital for health because it is an important fuel for physiological functions (58). Insulin is secreted by pancreatic β-cells and regulates the metabolism of glucose after food intake, increasing glucose uptake by skeletal muscle and adipose tissue and decreasing hepatic glucose production by blocking glycogenolysis and gluconeogenesis (59). The most important effect of insulin is the increase of glucose uptake, which can be mediated through AKT phosphorylation, which induces the translocation of GLUT4 to the plasma membrane (60–62). KO mice have increased glucose tolerance, insulin sensitivity, and liver gluconeogenesis. Part of these results is related to an increase in AKT phosphorylation in skeletal muscle and adipose tissues of KO in response to insulin stimulation. The lack of changes in liver AKT phosphorylation after insulin administration can be explained by the similar basal glycemia of KO and WT animals. KO mice exhibit more gluconeogenesis than WT animals, which is in accordance with the increased mRNA expression of specific genes that code for enzymes involved in gluconeogenesis in the liver (63–66). Moreover, *in silico* and experimental analyses corroborates that Nln is linked to energy metabolism and homeostasis regulation.

Accordingly, KO mice show alteration in mRNA expression of genes typical for slow twitch type I fibers (reduction of Tnni1, Tnnic1, Tnnt1, and Myh7), urea cycle (increase of CPSM), and glycolytic pathway (reduction of PGAM1/2) in the gastrocnemius but not in the soleus. Moreover, the histological analyses of SDH and COX in the gastrocnemius suggested a reduced mitochondrial oxidative activity. Several reports have shown that the skeletal muscle fiber composition is an important determinant in metabolism. Moreover, it is well established that slow twitch type I fibers act in glucose and lipid metabolism and endurance training promotes an increase of type I fiber muscles (67–72). Indeed, the KO mice ran less than WT mice in the low intensity running regime until exhaustion. Taken altogether, these results further suggest that Nln is linked to oxidative metabolic capacity.

Several previous reports correlated metabolic improvement with a lack of peptidase activity, suggesting that peptide metabolism plays an important function in homeostasis regulation (29, 30, 33). The phenotypic changes observed in the ACE transgenic mice are not affected by losartan, an antagonist of the angiotensin II receptor, suggesting that the renin-angiotensin system was likely not responsible for this phenotype (35). In contrast, Nln activity is significantly lower in the fat tissue of mice that possessed three copies of the ACE gene. A possible explanation for the latter observation is that ACE acts as a dipeptidyl-carboxypeptidase releasing dipeptides, which have been shown to specifically inhibit Nln (35). Reduced Nln activity in the fat tissue of ACE transgenic mice was associated with

the distinctive intracellular peptide profile of these ACE transgenic mice. These data let us propose that intracellular peptides could improve insulin sensitivity in the adipose tissue of ACE transgenic mice (35). Further investigation showed that the levels of specific intracellular peptides are increased in the adipose tissue of Wistar rats that were fed a high caloric Western diet, compared with rats fed a control diet. Two of these intracellular peptides (LDBI, GDVNTDRPGLLDL; and DBI, TVGDVNTDRPGLLDL) were reintroduced into 3T3-L1 adipocytes (treated or not with palmitate to induce insulin resistance) and shown to increase insulin-stimulated glucose uptake (36). These peptides were also shown to interact with specific proteins only in the adipose tissue from rats fed a high caloric Western diet (36), therefore suggesting that intracellular peptides could be endogenously involved in insulin-stimulated glucose uptake.

Previous biochemical, structural, and pharmacological evidence supports the high specificity of Nln for degrading small bioactive peptide substrates (9–11). Here, semiquantitative mass spectrometry analysis shows that specific intracellular peptides were affected in the KO compared with the WT mice. Therefore, it is likely that the phenotypes observed in the KO should be mediated by the lack of Nln enzymatic activity and, as a consequence, a shift in the intracellular peptide profile. A possible molecular mechanism related to intracellular peptide function includes binding to a protein and, as a consequence, modification of the ability of this protein to interact with other proteins. It is important to mention that intracellular peptides, distinctly from classical biologically active peptides, are suggested to function downstream of plasma membrane receptors, regulating signal transduction pathways from inside the cells (36, 47, 73, 74). Synthetic peptides have been extensively used to disrupt intracellular protein-protein interactions and alter protein functions. In some cases, synthetic peptides activate a protein by mimicking the effect of a protein-protein interaction; in other cases the peptides inhibit the protein by blocking a protein-protein interaction. Another possibility includes the binding of the peptide to a protein followed by alteration of its folding. Many proteins undergo conformational changes after binding to a peptide (75). It is possible that endogenous peptides perform similar functions as found for synthetic peptides (74). Indeed, genetic analysis of *Caenorhabditis elegans* shows that under stress of mitochondrial protein misfolding, peptide signals are emitted from the mitochondrial matrix to the nucleus, which regulate nuclear-encoded mitochondrial chaperone genes (76). Moreover, Thimet oligopeptidase inhibition using siRNA has been shown to affect β-adrenergic signal transduction in parallel to the intracellular peptide profile (73). Therefore, it is an exciting possibility to suggest that the phenotypes observed here in the KO mice are mediated by intracellular peptides caused by an oligopeptidase (77) action.

Nln have been suggested to participate in several important physiological processes like cardiovascular and renal homeostasis, pain perception, and regulation of the reproductive axis and recently also in the brain response to stroke (26, 28, 78–81). Also many studies using shRNA or chemical inhibitors supported the involvement of Nln in these physiological processes (24, 28, 78). Even though Nln is expressed widely in the central nervous system and peripheral organs of mammals (13, 83, 84), its absence, as shown here, is not lethal. KO mice reproduce normally and have normal blood pressure and heart rate when compared with WT mice. It has been previously suggested that *in vivo* Nln contributes to the metabolism of several endogenous peptides including neurotensin, bradykinin, angiotensins, substance P, opioids (*i.e.* metorphamide, dynorphin A_{1-8}), somatostatin, and hemopressin (5, 10, 26, 80). The presence of Nln activity in vascular endothelial cells suggested a possible physiological role for Nln in blood pressure control (79). However, even after neuropeptide injection (bradykinin, angiotensin II, and neurotensin), KO and WT mice have similar behaviors in blood pressure alterations. A parallel study conducted in our laboratory suggested that Nln knock-out only affects the levels of Met-enkephalin and octapeptide and thus exerts only a minor effect on intracellular peptide metabolism in the brain (82). Altogether, these data suggest that other peptidases may efficiently compensate the lack of Nln in physiological neuropeptide metabolism. However, further investigations are necessary to uncover the enzyme(s) involved in such compensatory mechanisms.

Acknowledgment—We thank Professor Lloyd D. Fricker for outstanding and helpful discussions during the manuscript preparation.

REFERENCES

1. Checler, F., Vincent, J. P., and Kitabgi, P. (1983) Degradation of neurotensin by rat brain synaptic membranes: involvement of a thermolysin-like metalloendopeptidase (enkephalinase), angiotensin-converting enzyme, and other unidentified peptidases. *J. Neurochem.* **41,** 375–384
2. Checler, F., Emson, P. C., Vincent, J. P., and Kitabgi, P. (1984) Inactivation of neurotensin by rat brain synaptic membranes. Cleavage at the Pro10-Tyr11 bond by endopeptidase 24.11 (enkephalinase) and a peptidase different from proline-endopeptidase. *J. Neurochem.* **43,** 1295–1301
3. Checler, F., Vincent, J. P., and Kitabgi, P. (1986) Purification and characterization of a novel neurotensin-degrading peptidase from rat brain synaptic membranes. *J. Biol. Chem.* **261,** 11274–11281
4. Ray, K., Hines, C. S., and Rodgers, D. W. (2002) Mapping sequence differences between Thimet oligopeptidase and neurolysin implicates key residues in substrate recognition. *Protein Sci.* **11,** 2237–2246
5. Rioli, V., Kato, A., Portaro, F. C., Cury, G. K., te Kaat, K., Vincent, B., Checler, F., Camargo, A. C., Glucksman, M. J., Roberts, J. L., Hirose, S., and Ferro, E. S. (1998) Neuropeptide specificity and inhibition of recombinant isoforms of the endopeptidase 3.4.24.16 family: comparison with the related recombinant endopeptidase 3.4.24.15. *Biochem. Biophys. Res. Commun.* **250,** 5–11
6. Rawlings, N. D., and Barrett, A. J. (1995) Evolutionary families of metallopeptidases. *Methods Enzymol.* **248,** 183–228
7. Ray, K., Hines, C. S., Coll-Rodriguez, J., and Rodgers, D. W. (2004) Crystal structure of human Thimet oligopeptidase provides insight into substrate recognition, regulation, and localization. *J. Biol. Chem.* **279,** 20480–20489
8. Barelli, H., Vincent, J. P., and Checler, F. (1993) Rat kidney endopeptidase 24.16. Purification, physico-chemical characteristics and differential specificity towards opiates, tachykinins and neurotensin-related peptides. *Eur. J. Biochem.* **211,** 79–90
9. Brown, C. K., Madauss, K., Lian, W., Beck, M. R., Tolbert, W. D., and Rodgers, D. W. (2001) Structure of neurolysin reveals a deep channel that limits substrate access. *Proc. Natl. Acad. Sci. U.S.A.* **98,** 3127–3132
10. Rioli, V., Gozzo, F. C., Heimann, A. S., Linardi, A., Krieger, J. E., Shida, C. S., Almeida, P. C., Hyslop, S., Eberlin, M. N., and Ferro, E. S. (2003) Novel natural peptide substrates for endopeptidase 24.15, neurolysin, and angiotensin-converting enzyme. *J. Biol. Chem.* **278,** 8547–8555
11. Dauch, P., Vincent, J. P., and Checler, F. (1995) Molecular cloning and

expression of rat brain endopeptidase 3.4.24.16. *J. Biol. Chem.* **270,** 27266–27271
12. Fontenele-Neto, J. D., Massarelli, E. E., Gurgel Garrido, P. A., Beaudet, A., and Ferro, E. S. (2001) Comparative fine structural distribution of endopeptidase 24.15 (EC 3.4.24.15) and 24.16 (EC 3.4.24.16) in rat brain. *J. Comp. Neurol.* **438,** 399–410
13. Massarelli, E. E., Casatti, C. A., Kato, A., Camargo, A. C., Bauer, J. A., Glucksman, M. J., Roberts, J. L., Hirose, S., and Ferro, E. S. (1999) Differential subcellular distribution of neurolysin (EC 3.4.24.16) and Thimet oligopeptidase (EC 3.4.24.15) in the rat brain. *Brain Res.* **851,** 261–265
14. Vincent, B., Beaudet, A., Dauch, P., Vincent, J. P., and Checler, F. (1996) Distinct properties of neuronal and astrocytic endopeptidase 3.4.24.16: a study on differentiation, subcellular distribution, and secretion processes. *J. Neurosci.* **16,** 5049–5059
15. Serizawa, A., Dando, P. M., and Barrett, A. J. (1995) Characterization of a mitochondrial metallopeptidase reveals neurolysin as a homologue of Thimet oligopeptidase. *J. Biol. Chem.* **270,** 2092–2098
16. Woulfe, J., Checler, F., and Beaudet, A. (1992) Light and electron microscopic localization of the neutral metalloendopeptidase EC 3.4.24.16 in the mesencephalon of the rat. *Eur. J. Neurosci.* **4,** 1309–1319
17. Garrido, P. A., Vandenbulcke, F., Ramjaun, A. R., Vincent, B., Checler, F., Ferro, E., and Beaudet, A. (1999) Confocal microscopy reveals Thimet oligopeptidase (EC 3.4.24.15) and neurolysin (EC 3.4.24.16) in the classical secretory pathway. *DNA Cell Biol.* **18,** 323–331
18. Kato, A., Sugiura, N., Saruta, Y., Hosoiri, T., Yasue, H., and Hirose, S. (1997) Targeting of endopeptidase 24.16 to different subcellular compartments by alternative promoter usage. *J. Biol. Chem.* **272,** 15313–15322
19. Jeske, N. A., Berg, K. A., Cousins, J. C., Ferro, E. S., Clarke, W. P., Glucksman, M. J., and Roberts, J. L. (2006) Modulation of bradykinin signaling by EP24.15 and EP24.16 in cultured trigeminal ganglia. *J. Neurochem.* **97,** 13–21
20. Doulut, S., Dubuc, I., Rodriguez, M., Vecchini, F., Fulcrand, H., Barelli, H., Checler, F., Bourdel, E., Aumelas, A., and Lallement, J. C. (1993) Synthesis and analgesic effects of N-[3-[(hydroxyamino) carbonyl]-1-oxo-2(*R*)-benzylpropyl]-L-isoleucyl-L-leucine, a new potent inhibitor of multiple neurotensin/neuromedin N degrading enzymes. *J. Med. Chem.* **36,** 1369–1379
21. Barelli, H., Fox-Threlkeld, J. E., Dive, V., Daniel, E. E., Vincent, J. P., and Checler, F. (1994) Role of endopeptidase 3.4.24.16 in the catabolism of neurotensin, *in vivo*, in the vascularly perfused dog ileum. *Br. J. Pharmacol.* **112,** 127–132
22. Oliveira, E. B., Souza, L. L., Sivieri, D. O., Jr., Bispo-da-Silva, L. B., Pereira, H. J., Costa-Neto, C. M., Sousa, M. V., and Salgado, M. C. (2007) Carboxypeptidase B and other kininases of the rat coronary and mesenteric arterial bed perfusates. *Am. J. Physiol. Heart Circ. Physiol.* **293,** H3550–H3557
23. Blais, P. A., Côté, J., Morin, J., Larouche, A., Gendron, G., Fortier, A., Regoli, D., Neugebauer, W., and Gobeil, F., Jr. (2005) Hypotensive effects of hemopressin and bradykinin in rabbits, rats and mice: a comparative study. *Peptides* **26,** 1317–1322
24. Piliponsky, A. M., Chen, C. C., Nishimura, T., Metz, M., Rios, E. J., Dobner, P. R., Wada, E., Wada, K., Zacharias, S., Mohanasundaram, U. M., Faix, J. D., Abrink, M., Pejler, G., Pearl, R. G., Tsai, M., and Galli, S. J. (2008) Neurotensin increases mortality and mast cells reduce neurotensin levels in a mouse model of sepsis. *Nat. Med.* **14,** 392–398
25. Dauch, P., Masuo, Y., Vincent, J. P., and Checler, F. (1992) Endopeptidase 24–16 in murines: tissue distribution, cerebral regionalization, and ontogeny. *J. Neurochem.* **59,** 1862–1867
26. Shrimpton, C. N., Smith, A. I., and Lew, R. A. (2002) Soluble metalloendopeptidases and neuroendocrine signaling. *Endocr. Rev.* **23,** 647–664
27. Paschoalin, T., Carmona, A. K., Rodrigues, E. G., Oliveira, V., Monteiro, H. P., Juliano, M. A., Juliano, L., and Travassos, L. R. (2007) Characterization of Thimet oligopeptidase and neurolysin activities in B16F10-Nex2 tumor cells and their involvement in angiogenesis and tumor growth. *Mol. Cancer* **6,** 44
28. Rashid, M., Wangler, N. J., Yang, L., Shah, K., Arumugam, T. V., Abbruscato, T. J., and Karamyan, V. T. (2014) Functional upregulation of endopeptidase neurolysin during post-acute and early recovery phases of experimental stroke in mouse brain. *J. Neurochem.* **129,** 179–189
29. Mest, H. J., and Mentlein, R. (2005) Dipeptidyl peptidase inhibitors as new drugs for the treatment of type 2 diabetes. *Diabetologia* **48,** 616–620
30. Tagore, D. M., Nolte, W. M., Neveu, J. M., Rangel, R., Guzman-Rojas, L., Pasqualini, R., Arap, W., Lane, W. S., and Saghatelian, A. (2009) Peptidase substrates via global peptide profiling. *Nat. Chem. Biol.* **5,** 23–25
31. Barros, C. C., Haro, A., Russo, F. J., Schadock, I., Almeida, S. S., Reis, F. C., Moraes, M. R., Haidar, A., Hirata, A. E., Mori, M., Bacurau, R. F., Würtele, M., Bader, M., Pesquero, J. B., and Araujo, R. C. (2012) Bradykinin inhibits hepatic gluconeogenesis in obese mice. *Lab. Invest.* **92,** 1419–1427
32. Barros, C. C., Haro, A., Russo, F. J., Schadock, I., Almeida, S. S., Ribeiro, R. A., Vanzela, E. C., Lanzoni, V. P., Barros, F. C., Moraes, M. R., Mori, M. A., Bacurau, R. F., Wurtele, M., Boschero, A. C., Carneiro, E. M., Bader, M., Pesquero, J. B., and Araujo, R. C. (2012) Altered glucose homeostasis and hepatic function in obese mice deficient for both kinin receptor genes. *PLoS One* **7,** e40573
33. Anubhuti, and Arora, S. (2008) Leptin and its metabolic interactions: an update. *Diabetes Obes. Metab.* **10,** 973–993
34. Naggert, J. K., Fricker, L. D., Varlamov, O., Nishina, P. M., Rouille, Y., Steiner, D. F., Carroll, R. J., Paigen, B. J., and Leiter, E. H. (1995) Hyperproinsulinaemia in obese fat/fat mice associated with a carboxypeptidase E mutation which reduces enzyme activity. *Nat. Genet.* **10,** 135–142
35. Heimann, A. S., Favarato, M. H., Gozzo, F. C., Rioli, V., Carreño, F. R., Eberlin, M. N., Ferro, E. S., Krege, J. H., and Krieger, J. E. (2005) ACE gene titration in mice uncovers a new mechanism for ACE on the control of body weight. *Physiol. Genomics* **20,** 173–182
36. Berti, D. A., Russo, L. C., Castro, L. M., Cruz, L., Gozzo, F. C., Heimann, J. C., Lima, F. B., Oliveira, A. C., Andreotti, S., Prada, P. O., Heimann, A. S., and Ferro, E. S. (2012) Identification of intracellular peptides in rat adipose tissue: insights into insulin resistance. *Proteomics* **12,** 2668–2681
37. Dauch, P., Vincent, J. P., and Checler, F. (1991) Specific-inhibition of endopeptidase-24.16 by dipeptides. *Eur. J. Biochem.* **202,** 269–276
38. Castro, C. H., Shin, C. S., Stains, J. P., Cheng, S. L., Sheikh, S., Mbalaviele, G., Szejnfeld, V. L., and Civitelli, R. (2004) Targeted expression of a dominant-negative N-cadherin *in vivo* delays peak bone mass and increases adipogenesis. *J. Cell Sci.* **117,** 2853–2864
39. Kang, K., Reilly, S. M., Karabacak, V., Gangl, M. R., Fitzgerald, K., Hatano, B., and Lee, C. H. (2008) Adipocyte-derived Th2 cytokines and myeloid PPARδ regulate macrophage polarization and insulin sensitivity. *Cell Metab.* **7,** 485–495
40. Lagouge, M., Argmann, C., Gerhart-Hines, Z., Meziane, H., Lerin, C., Daussin, F., Messadeq, N., Milne, J., Lambert, P., Elliott, P., Geny, B., Laakso, M., Puigserver, P., and Auwerx, J. (2006) Resveratrol improves mitochondrial function and protects against metabolic disease by activating SIRT1 and PGC-1α. *Cell* **127,** 1109–1122
41. Yamamoto, H., Williams, E. G., Mouchiroud, L., Cantó, C., Fan, W., Downes, M., Héligon, C., Barish, G. D., Desvergne, B., Evans, R. M., Schoonjans, K., and Auwerx, J. (2011) NCoR1 is a conserved physiological modulator of muscle mass and oxidative function. *Cell* **147,** 827–839
42. Cardoso, C. C., Alenina, N., Ferreira, A. J., Qadri, F., Lima, M. P., Gross, V., Todiras, M., Pesquero, J. B., Pesquero, J. L., and Bader, M. (2010) Increased blood pressure and water intake in transgenic mice expressing rat tonin in the brain. *Biol. Chem.* **391,** 435–441
43. Cayla, C., Todiras, M., Iliescu, R., Saul, V. V., Gross, V., Pilz, B., Chai, G., Merino, V. F., Pesquero, J. B., Baltatu, O. C., and Bader, M. (2007) Mice deficient for both kinin receptors are normotensive and protected from endotoxin-induced hypotension. *FASEB J.* **21,** 1689–1698
44. Castro, L. M., Berti, D. A., Russo, L. C., Coelho, V., Gozzo, F. C., Oliveira, V., and Ferro, E. S. (2010) Similar intracellular peptide profile of TAP1/β2 microglobulin double-knockout mice and C57BL/6 wild-type mice as revealed by peptidomic analysis. *AAPS J.* **12,** 608–616
45. Fricker, L. D., Gelman, J. S., Castro, L. M., Gozzo, F. C., and Ferro, E. S. (2012) Peptidomic analysis of HEK293T cells: effect of the proteasome inhibitor epoxomicin on intracellular peptides. *J. Proteome Res.* **11,** 1981–1990
46. Udenfriend, S., Stein, S., Böhlen, P., Dairman, W., Leimgruber, W., and Weigele, M. (1972) Fluorescamine: a reagent for assay of amino acids, peptides, proteins, and primary amines in the picomole range. *Science* **178,** 871–872

47. Cunha, F. M., Berti, D. A., Ferreira, Z. S., Klitzke, C. F., Markus, R. P., and Ferro, E. S. (2008) Intracellular peptides as natural regulators of cell signaling. *J. Biol. Chem.* **283,** 24448–24459
48. Fricker, L. D. (2010) Analysis of mouse brain peptides using mass spectrometry-based peptidomics: implications for novel functions ranging from non-classical neuropeptides to microproteins. *Mol. Biosyst.* **6,** 1355–1365
49. Gelman, J. S., Sironi, J., Castro, L. M., Ferro, E. S., and Fricker, L. D. (2011) Peptidomic analysis of human cell lines. *J. Proteome Res.* **10,** 1583–1592
50. Maere, S., Heymans, K., and Kuiper, M. (2005) BiNGO: a Cytoscape plugin to assess overrepresentation of gene ontology categories in biological networks. *Bioinformatics* **21,** 3448–3449
51. Shannon, P., Markiel, A., Ozier, O., Baliga, N. S., Wang, J. T., Ramage, D., Amin, N., Schwikowski, B., and Ideker, T. (2003) Cytoscape: a software environment for integrated models of biomolecular interaction networks. *Genome Res.* **13,** 2498–2504
52. Rice, J. A. (2007) *Mathematical Statistics and Data Analysis*, 3rd Ed., Duxbury Press, Pacific Grove, CA
53. Benjamini, Y., and Yekutieli, D. (2001) The control of the false discovery rate in multiple testing under dependency. *Ann. Stat.* **29,** 1165–1188
54. Hernandez-Toro, J., Prieto, C., and De las Rivas, J. (2007) APID2NET: unified interactome graphic analyzer. *Bioinformatics* **23,** 2495–2497
55. Panico, K., and Forti, F. L. (2013) Proteomic, cellular, and network analyses reveal new DUSP3 interactions with nucleolar proteins in HeLa cells. *J. Proteome Res.* **12,** 5851–5866
56. Checler, F. (2014) Experimental stroke: neurolysin back on stage. *J. Neurochem.* **129,** 1–3
57. Haffner, S. M., D'Agostino, R., Jr., Mykkänen, L., Tracy, R., Howard, B., Rewers, M., Selby, J., Savage, P. J., and Saad, M. F. (1999) Insulin sensitivity in subjects with type 2 diabetes. Relationship to cardiovascular risk factors: the Insulin Resistance Atherosclerosis Study. *Diabetes Care* **22,** 562–568
58. Richter, E. A., and Hargreaves, M. (2013) Exercise, GLUT4, and skeletal muscle glucose uptake. *Physiol. Rev.* **93,** 993–1017
59. Saltiel, A. R., and Kahn, C. R. (2001) Insulin signalling and the regulation of glucose and lipid metabolism. *Nature* **414,** 799–806
60. Tan, S. X., Ng, Y., and James, D. E. (2010) Akt inhibitors reduce glucose uptake independently of their effects on Akt. *Biochem. J.* **432,** 191–197
61. Tian, R. (2005) Another role for the celebrity Akt and insulin resistance. *Circ. Res.* **96,** 139–140
62. Ng, Y., Ramm, G., Lopez, J. A., and James, D. E. (2008) Rapid activation of Akt2 is sufficient to stimulate GLUT4 translocation in 3T3-L1 adipocytes. *Cell Metab.* **7,** 348–356
63. Mayr, B., and Montminy, M. (2001) Transcriptional regulation by the phosphorylation-dependent factor CREB. *Nat. Rev. Mol. Cell Biol.* **2,** 599–609
64. Jitrapakdee, S. (2012) Transcription factors and coactivators controlling nutrient and hormonal regulation of hepatic gluconeogenesis. *Int. J. Biochem. Cell Biol.* **44,** 33–45
65. Authier, F., and Desbuquois, B. (2008) Glucagon receptors. *Cell Mol. Life Sci.* **65,** 1880–1899
66. Corssmit, E. P., Romijn, J. A., and Sauerwein, H. P. (2001) Regulation of glucose production with special attention to nonclassical regulatory mechanisms: a review. *Metabolism* **50,** 742–755
67. Nader, G. A., and Esser, K. A. (2001) Intracellular signaling specificity in skeletal muscle in response to different modes of exercise. *J. Appl Physiol.* **90,** 1936–1942
68. Williamson, D. L., Gallagher, P. M., Carroll, C. C., Raue, U., and Trappe, S. W. (2001) Reduction in hybrid single muscle fiber proportions with resistance training in humans. *J. Appl. Physiol.* **91,** 1955–1961
69. Fritah, A., Steel, J. H., Parker, N., Nikolopoulou, E., Christian, M., Carling, D., and Parker, M. G. (2012) Absence of RIP140 reveals a pathway regulating glut4-dependent glucose uptake in oxidative skeletal muscle through UCP1-mediated activation of AMPK. *PLoS One* **7,** e32520
70. Izumiya, Y., Hopkins, T., Morris, C., Sato, K., Zeng, L., Viereck, J., Hamilton, J. A., Ouchi, N., LeBrasseur, N. K., and Walsh, K. (2008) Fast/glycolytic muscle fiber growth reduces fat mass and improves metabolic parameters in obese mice. *Cell Metab.* **7,** 159–172
71. Wang, Y. X., Zhang, C. L., Yu, R. T., Cho, H. K., Nelson, M. C., Bayuga-Ocampo, C. R., Ham, J., Kang, H., and Evans, R. M. (2004) Regulation of muscle fiber type and running endurance by PPARδ. *PLoS Biol.* **2,** e294
72. Abou Mrad, J., Yakubu, F., Lin, D., Peters, J. C., Atkinson, J. B., and Hill, J. O. (1992) Skeletal muscle composition in dietary obesity-susceptible and dietary obesity-resistant rats. *Am. J. Physiol.* **262,** R684–R688
73. Russo, L. C., Castro, L. M., Gozzo, F. C., and Ferro, E. S. (2012) Inhibition of Thimet oligopeptidase by siRNA alters specific intracellular peptides and potentiates isoproterenol signal transduction. *FEBS Lett.* **586,** 3287–3292
74. Ferro, E. S., Rioli, V., Castro, L. M., and Fricker, L. D. (2014) Intracellular peptides: from discovery to function. *EuPA Open Proteomics* **3,** 143–151
75. Arkin, M. R., and Whitty, A. (2009) The road less traveled: modulating signal transduction enzymes by inhibiting their protein-protein interactions. *Curr. Opin. Chem. Biol.* **13,** 284–290
76. Haynes, C. M., Yang, Y., Blais, S. P., Neubert, T. A., and Ron, D. (2010) The matrix peptide exporter HAF-1 signals a mitochondrial UPR by activating the transcription factor ZC376.7 in C. elegans. *Mol. Cell* **37,** 529–540
77. Oliveira EB, Martins AR, Camargo AC (1976) Isolation of brain endopeptidases: influence of size and sequence of substrates structurally related to bradykinin. *Biochemistry* **15,** 1967–1974
78. Smith, A. I., Lew, R. A., Shrimpton, C. N., Evans, R. G., and Abbenante, G. (2000) A novel stable inhibitor of endopeptidases EC 3.4.24.15 and 3.4.24.16 potentiates bradykinin-induced hypotension. *Hypertension* **35,** 626–630
79. Norman, M. U., Reeve, S. B., Dive, V., Smith, A. I., and Lew, R. A. (2003) Regulation of cardiovascular signaling by kinins and products of similar converting enzyme systems: endopeptidases 3.4.24.15 and 24.16 in endothelial cells: potential role in vasoactive peptide metabolism. *Am. J. Physiol. Heart Circ. Physiol.* **284,** H1978–H1984
80. Norman, M. U., Reeve, S. B., Dive, V., Smith, A. I., and Lew, R. A. (2003) Endopeptidases 3.4.24.15 and 24.16 in endothelial cells: potential role in vasoactive peptide metabolism. *Am. J. Physiol. Heart Circ. Physiol.* **284,** H1978–H1984
81. Vincent, B., Jiracek, J., Noble, F., Loog, M., Roques, B., Dive, V., Vincent, J. P., and Checler, F. (1997) Effect of a novel selective and potent phosphinic peptide inhibitor of endopeptidase 3.4.24.16 on neurotensin-induced analgesia and neuronal inactivation. *Br. J. Pharmacol.* **121,** 705–710
82. Castro, L. M., Cavalcanti, D. M., Araujo, C. B., Rioli, V., Icimoto, M. Y., Gozzo, F. C., Juliano, M., Juliano, L., Oliveira, V., Ferro, E. S. (2014) Peptidomic analysis of the neurolysin-knockout mouse brain. *J. Proteomics* 10.1016/j.jprot.2014.03.043
83. Krause, D. R., Piva, T. J., Brown, S. B., and Ellem, K. A. (1997) Characterization and localization of mitochondrial oligopeptidase (MOP) (EC 3.4.24.16) activity in the human cervical adenocarcinoma cell line HeLa. *J. Cell. Biochem.* **66,** 297–308
84. Barrett, A. J., Brown, M. A., Dando, P. M., Knight, C. G., McKie, N., Rawlings, N. D., and Serizawa, A. (1995) Thimet oligopeptidase and oligopeptidase-M or neurolysin. *Methods Enzymol.* **248,** 529–556
85. Benjamini, Y., and Hochberg, Y. (1995) Controlling the false discovery rate: practical and powerful approach to multiple testing. *J. R. Stat. Soc. Series B Stat. Methodol.* **57,** 289–300